QUASIELASTIC DISTRIBUTIONS FOR TRANSVERSE KINEMATIC VARIABLES

A THESIS
SUBMITTED TO THE FACULTY OF THE GRADUATE SCHOOL
OF THE UNIVERSITY OF MINNESOTA
BY

LAUREN ALEXANDRIA HAREWOOD

IN PARTIAL FULFILLMENT OF THE REQUIREMENTS
FOR THE DEGREE OF
MASTER OF SCIENCE

RICHARD GRAN, Adviser

JUNE 2019

Acknowledgements

To Source: Thank you. I know that this is exactly where I was supposed to be.

To my mother: Thank you for everything. I am so lucky to have you.

To my grandmother Julia Mae Middleton: I am so happy you are turning ninety. I'm coming home!

To GG: Thank you. Ase.

Alexis Octavia: You are so excellent, always an inspiration, always progressing.

To Aunt Mindy: Thanks for the kind words and support.

To Uncle Lincoln: You passed just before I moved back to the States. I never got to tell you how grateful I am for you helping to raise me. I miss you so much.

To Uncle Robert: You passed the week before my thesis was due. I am so sorry I didn't get a chance to say goodbye. Goodbye handsome man!

To Dad: Thanks for all the support!

To MINERvA students and faculty: Thank you for your kindness and welcoming spirits.

To Joe Gallian: You are by far the best teacher I have ever had. I am really inspired by your work ethic and easygoing, nurturing spirit.

To Dr Habig: Thank you for your kindness. It really helped me feel more comfortable in Duluth.

To Dr Gran: Thank you. You were a great advisor.

Dedication

For Julia Mae Middleton

Abstract

The MINERvA experiment, located at the Fermi National Accelerator Laboratory (Illinois), is a detector designed to study neutrino-nuclear interactions. MINERvA has been instrumental in understanding how neutrinos interact with nuclei and its research has been used to better analyze data from oscillation experiments like MicroBooNE, DUNE (Deep Underground Neutrino Experiment) and NOvA (NuMi Off Axis v Appearance) and prepare for the future experiment DUNE. Though MINERvA has ended data collection this year, more analysis on the models of nuclear interaction happening in the nucleus is required. GENIE, a neutrino event generator, is one used to model such interactions. Upon reviewing special features in transverse kinematic distributions, the task, a flaw in a part of the model affecting nearly all interactions was found and fixed. In this study, a new GENIE simulation of a class of quasielastic neutrino events will be presented, along with results for the new transverse kinematic imbalance distributions. An approximate fix is proposed for already generated samples of simulated events.

Contents

List of Tables

List of Figures

1 Introduction

Neutrinos, a type of elementary particle, and properties related to their mass are a hotly researched topics in modern particle physics. Cutting edge research is conducted globally at world-class laboratories with Fermilab in the U.S, CERN in Europe, and T2K in Japan at the forefront. This thesis evaluates models for neutrino interactions in nuclei and also proton interactions in nuclei. Modeling the former using the latter is the subject of the current writeup.

Neutrino-nuclei interactions are crucial for interpreting data from neutrino oscillation experiments. Since neutrinos are the second most common particle in the universe, the overall program has the potential to change how we understand the fundamental structure of the universe.

The work here focuses on a fix to a portion of the neutrino event generating simulation. The new code produces significant changes in the distributions for certain so-called "transverse kinematic imbalance observables." This thesis discusses the formulation of the fix, the resulting distributions, and a recommendation for implementing the fix.

The original model made some predictions difficult to understand. My early studies were predicated on looking for an unexpected physics effect. Predicting and explaining where the effect was coming from could mean more ways to measure the effect. Since the issues were later identified as a bug, that early work was no longer relevant. They are not included in this thesis, though this work builds from those original studies.

The Standard Model The Standard Model of Particle Physics is a theory which explains how the four fundamental forces come to be through the fields of elementary particles. The theory describes these particles and the types of interactions in which they participate. The standard model has great predictive abilities, but is seen as incomplete. Neutrino mass, in particular, presents a unique challenge to the model.

The work here is primarily about neutrino interactions with neutrons (udd quarks) with a zero net charge turning into protrons (uud quarks) which have net positive charge. These interactions also turn the muon neutrinos ν_μ into muons μ^-. This special subset of interactions monitored by neutrino physicists is the key concern of the current thesis.

1.0.1 Forces and carrier particles

There are four types of fundamental interactions, or forces, in the universe — the electromagnetic, gravity, strong, and weak. Of the four gravity is the weakest but has an infinite range. The electromagnetic force is the next strongest, also with infinite range. The weak and strong interactions which have range only at the level of subatomic particles. The weak force is stronger than gravity. The strong force is the strongest of all four fundamental interactions.

Three of the fundamental forces result from known force-carrier particles called bosons. Matter particles transfer energy and momentum with each other through the exchange of bosons. Each fundamental force has its own: the electromagnetic force=the photon, strong=the gluon, weak=the W and Z bosons. The standard model does not account for gravity, but the graviton, or gravity particle, is believed to be the boson responsible for carrying the gravitational interaction while the Higgs is believed to be the origin of mass in the theory. The graviton has not been found.

The weak force, like all forces, causes a momentum transfer between two objects. The momentum transfer is mathematically equivalent to physically exchanging a particle. When neutrinos interact via the weak force, they exchange W or Z bosons.

Protons and neutrons interact via the strong or weak force but when they interact with each other, the strong force is much more important. The strong force which holds the nucleus together is often mediated through the exchange of $q\bar{q}$ pairs such as “pions” which are also bosons. This study will focus on the cases when weak

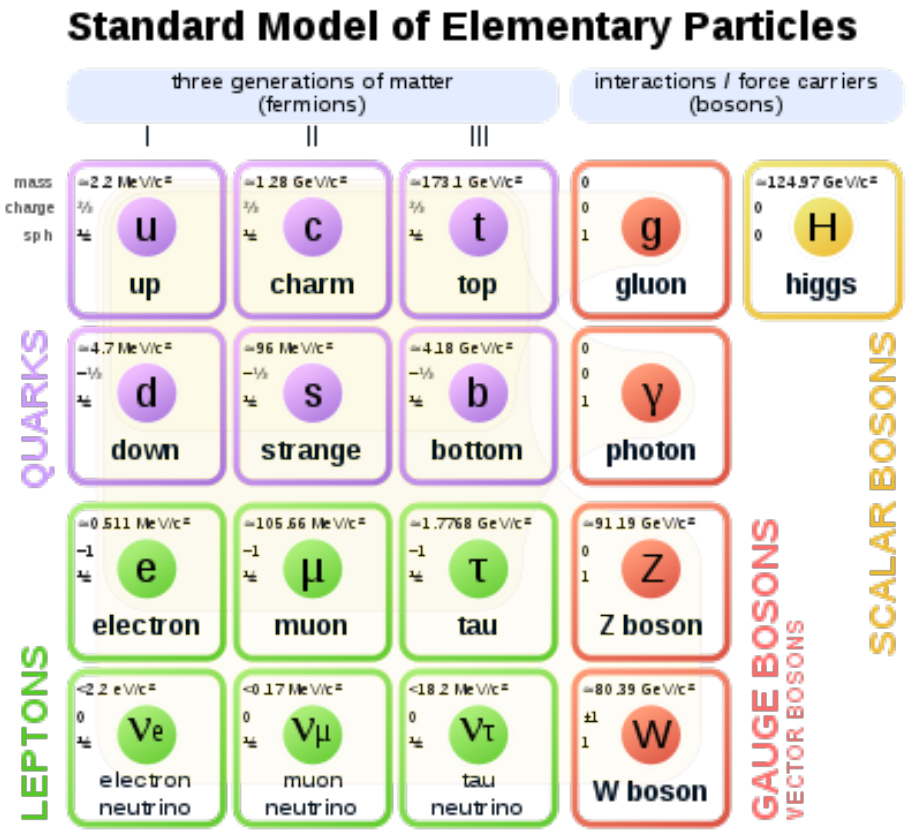

Figure 1: Figure above shows Standard Model of Particle Physics. Fermions, spin 1/2 particles come in pairs of 3 generations. Quarks have partial charge. Up, Charm, and Top have a $+2/3 \times$ elementary charge, while down, strange,and bottom have $-1/3 \times$ elementary charge. The gauge bosons, spin 1 particles, are the force carriers in the model. Exchange of these bosons results in the electromagnetic (γ), weak (Z and W), and strong (gluon) interactions. The gluon and W particles are charged while the Z, γ are uncharged. Neutrinos, represented by ν are also not electrically charged. The Higgs was observed for the first time at the LHC at CERN. Each particle also has a corresponding antiparticle of opposite charge. The antiparticles are not pictured. Diagram from [13].

interactions in nuclei are followed by a strong force interaction in the same nucleus to produce the final outcome.

1.0.2 Matter Particles

All matter is made up of two types of elementary particles, quarks and leptons. These particles are categorized into three generations. The first generation, made of the least massive particles, comprise the stable matter in the universe. Referring to Figure 1 the first two rows are quarks while the last two are leptons. The first three columns are the three generations of matter.

Stable matter, like nuclei, are nearly always first generation up and down quarks (in neutrons and protons) plus electrons. These particles are also matter rather than antimatter and comprise the material of which our detectors are made. The second and third generations contain the heavier, less-stable particles. The beam contains the second generation lepton ν_μ.

The six quarks come in three generations. The first generation consists of the up and down quarks while the second and third comprise the strange and charm, top and bottom quarks, respectively. These quarks also come in three "colors" to form "colorless" bound states called hadrons or mesons. The six leptons are also categorized in three generations-the electron and the electron neutrino, the muon, and the muon neutrino, and the tau and the tau neutrino. The electron, muon, and tau all have mass and electric charge, while neutrinos are electrically neutral and have very small masses.

1.1 Neutrinos

Neutrinos have become the topic of much discussion in nuclear and particle physics. Neutrinos are believed to be the second most abundant particle in nature, after photons. At any given moment, millions of neutrinos are passing through you, originating from all over the known universe. Still, little is known about them. Since they are chargeless, they do not interact with matter easily and it would take a thousand years for the reader to have a neutrino interact with their body.

What we do know is that neutrinos come in three "flavors"-electron, mu, and tau, corresponding to the types of leptonic interactions in which they participate. Interactions preserve flavour. This means a muon neutrino does not become an electron or a tau in any reaction.

Currently, it is not clear whether neutrinos have a distinct antiparticle. Whether neutrinos are Dirac (distinct $\bar{\nu}$) or Majorana ($\bar{\nu}$ and ν are the same particle) may have important implications for available quantum states for the neutrino and special symmetry conservation theories.

Turns out that as they travel neutrinos may also change their flavour, or "oscillate". According to the standard model neutrinos should not have mass, but the phenomenon of flavor oscillation requires the existence of neutrino mass. In order to change flavour with time, to experience time at all, special relativity requires neutrinos to have mass. They also need a quantum mechanical mechanism where flavour states are a superposition of mass states and vice versa.

We know that there are three neutrino mass states, which when mixed together form the three flavour states. The Nobel prize was awarded to Takaaki Kajita and Arthur B McDonald in 2015 for proving their experimental discovery of neutrino oscillation. However, we still do not know exactly what these masses are or how they are ordered. Doing this requires more precise measurements of both neutrino-nucleus interactions and the approximation of such interactions.

1.2 Units

Units can get cumbersome in physics. In this thesis I will use the standard elementary particle physics set. Energy is in GeV or MeV rather than the usual Joules or $\frac{kgm^2}{s^2}$. One eV is the energy required to raise the electric potential of an electron or proton by one volt. Momentum is in GeV/c or MeV/c, not $\frac{kgm}{s}$. Mass is GeV/c^2 or MeV/c^2, not kg.

1.3 Interactions According to Standard Model

This section is included to help the reader understand how fermions, the matter particles, may change identity after exchanging a carrier particle. Once hadrons participate in a weak interaction with a lepton their quark content may change. This allows for a wide array of possibilities in outcomes as long as specific quantities are conserved.

1.3.1 Lepton Number and Baryon Number Conservation

All known experimental data show that the interactions of the electron and its neutrino are identical to those of the muon and its neutrino and the tauon and its neutrino. Each generation of lepton has a lepton number associated with it. The electron number is the number of electrons (e^-) and electron neutrinos (ν_e) minus the number of positrons (antielectron-e^+) and antielectron neutrinos ($\bar{\nu_e}$). The conservation is summarized as

$$L_e = N(e^-) - N(e^+) + N(\nu_e) - N(\bar{\nu_e}) \tag{1}$$

$$L_\mu = N(\mu^-) - N(\mu^+) + N(\nu_\mu) - N(\bar{\nu_\mu}) \tag{2}$$

$$L_\tau = N(\tau^-) - N(\tau^+) + N(\nu_\tau) - N(\bar{\nu_\tau}) \tag{3}$$

where N (l) is number of that particular lepton or antilepton in the interaction.

In the following discussion we assume the simple quark model in which only three simplest types of quark bound states are possible- the baryons (with structure qqq), antibaryons ($\bar{q}\bar{q}\bar{q}$), and mesons (q$\bar{q}$) $q - quark, \bar{q} - antiquark$. Baryon number is a measure of the number of quarks rather than antiquarks a baryon has. Baryons have baryon number 1, antibaryons -1, and mesons 0.

$$B \equiv (1/3)[N(q) - N(\bar{q})] \tag{4}$$

where N (q) is the number of quarks or antiquarks in the interaction

In the standard model, all known interactions conserve each lepton number individually. Lepton flavour conservation is violated where neutrino oscillation occurs.

There are searches for additional oddities like charged lepton flavour violation and Majorana neutrinos.

For strong interaction processes the final state contains the same number of quarks of each flavor as the initial state. For example, the process which creates an antineutron and neutron from a proton and an antiproton.

$$p(uud) + \bar{p}(\bar{u}\bar{u}\bar{d}) \longrightarrow n(udd) + \bar{n}(\bar{u}\bar{d}\bar{d}) \tag{5}$$

In this interaction baryon number is conserved. In the initial state there are 0 total up quarks (up and antiup cancel) and 0 total down quarks.

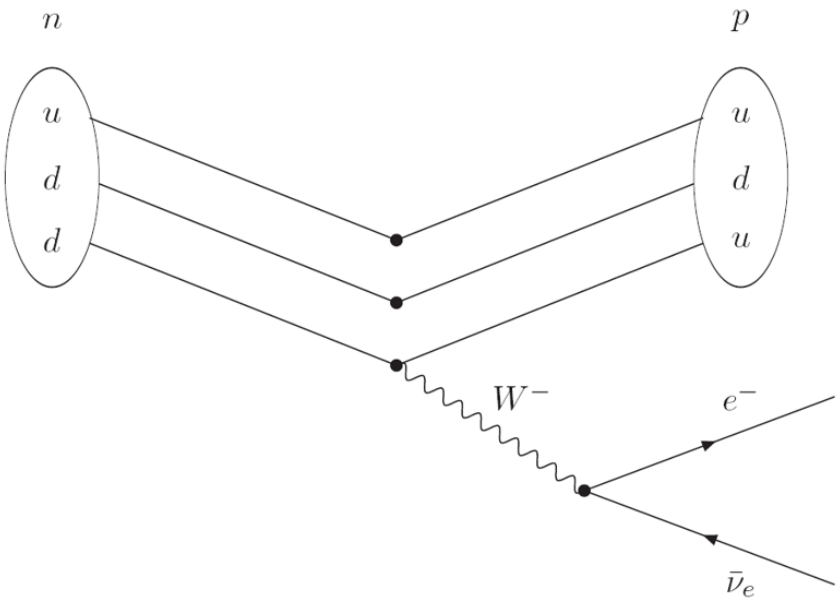

Figure 2: Feynman diagram of neutron beta decay into proton electron, and anti-electron neutrino. Down quark becomes an up quark after exchanging momentum with W. The W boson takes negative charge away and leaves a proton behind. Time moves to the right in this diagram. Diagram from [18].

However, for some weak processes, like the decay of a long-lived neutron or hadron, the quark flavor can change. An example is beta decay- the process (shown in Figure 2) that led to the discovery of the neutrino. A W boson is released (or scattered off of) and a quark changes flavor. The neutron releases the W and the W carries away a minus charge and some momentum from the neutron to create the electron and leave behind a proton and an antielectron neutrino and an electron.

Lepton number is conserved. It is zero before the W is exchanged and zero after. Baryon number is conserved. It is one before collision and one after. Energy is also conserved because n is more massive that ν_e, e^- and p.

1.3.2 Charged Current/Neutral Current Scattering

Weak decay is only one example of a weak process. There are also weak processes that result from a lepton-hadron scatter. In Figure 3 the weak interaction studied in this thesis is shown. The W changes the flavour of the quarks in the hadron leaving baryon number the same. The lepton becomes another lepton conserving lepton number at one.

Charged current scattering interactions are those in which a charged boson is exchanged. For hadrons this leads to a flavor change. For example, when a down quark interacts with a W and becomes an up quark the hadron it was a part of also changes e.g. from a neutron to a proton. The neutral current reactions do not exchange charge nor any quark flavors. The original baryon may still be in its ground or an excited state. In all cases, momentum, spin, and energy are exchanged.

Therefore, we can distinguish between these types of weak interactions,inferring which boson must have been exchanged, by looking at the outcome of the reaction. The interaction ν_μ + n $\longrightarrow$ μ^- + p is a charged current reaction. We know this because to turn a neutron into a proton we must have a flavor change occur and there a Z does cannot carry charge nor does it change flavour.

1.3.3 ν + C , p + C

In heavy ion experiments a hadron beam can be scattered off of a nuclear target, or hadrons collide with each other. There are also neutrino-nucleus experiments the make a neutrino beam scatter off of with a fixed target nucleus. The hadron-nucleus or hadron-nucleon interactions are mediated by the strong force while the neutrino-nucleus interactions occur via the weak force.

In addition to interacting with a single one of the 12 nucleons in carbon individually (knocking it out), the interaction can happen with the nucleus as a whole. In this case, the nucleus remains unchanged or maybe in a collective excited state after the reaction, with no nucleons knocked out. For strong force, hadron-nucleus reactions this is called elastic scattering. It is this part of the model that was fixed.

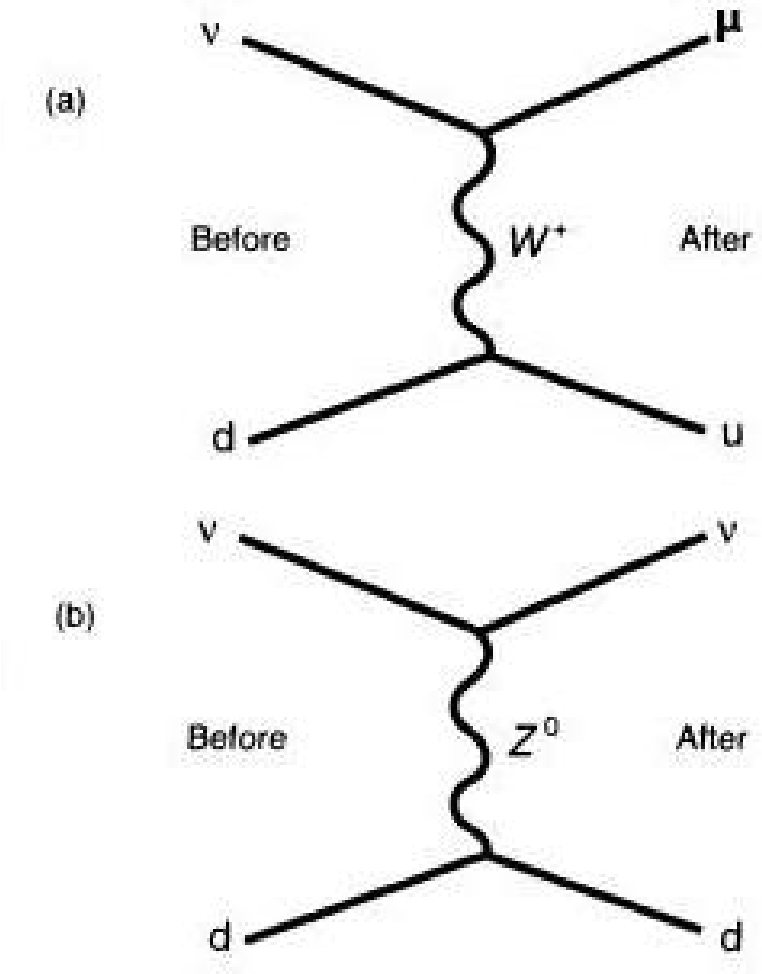

Figure 3: Feynman diagrams of charged current and neutral current weak interactions. a) the down quark becomes an up quark and the neutrino becomes a negatively charged lepton. b) neutrino exchanges neutral Z boson with a down quark. The down quark is unchanged and the neutrino continues on its way. Diagram from [2].

1.4 Motivation

Most of our knowledge of the subnuclear world comes from high energy experiments. By analyzing the outgoing particles, their energies, and momenta the nuclear physics community has been able to stitch together some key understandings about the nature of interactions at these very short, 10^{-15} m distances. Since the length scales are so small,in the subatomic world interactions are governed by quantum mechanics.

One cannot speak with certainty about the outcome of any collision before it happens. One can only speak in terms of probabilities of certain products being produced, or certain interactions occurring. These probabilities can sometimes be calculated from theory, maybe with unknown or uncertain parameters, and they can be measured. Modern experiments collect large amounts of data on various interactions which are analyzed by teams of dozens to hundreds of scientists.

The number of events with special properties within the collected data set is proportional to the probability of such an event. So the probability of measuring a certain outcome (proportional to what is called the cross section) of a collision, connects theoretical predictions to experiment. In this thesis, most of these probabilities are shown strictly in terms of number of events from a sample of fixed size– one million simulated reactions.

1.4.1 Need for Increased Experimental Precision in Neutrino-Nucleus Events

The analysis tools for studying these events have become more advanced, while more and more sophisticated, computer-driven, high channel count data acquisition systems are also commonplace. However, the detectors and experiment design have not changed much since the 70 s. MINERvA has a more traditional, tried and true setup. Until recently most experiments on neutrino-nucleus interaction had carbon, iron, or, water targets, because they were the least expensive way to build huge detectors.

The newest experiments will mostly use liquid argon as a detection medium. This is largely due to both the impressive experimental precision associated with the device known as a time projection chamber, especially when filled with liquid argon, and the economic ease of procuring argon, which is one percent of air.

The MINERvA experiment is analyzing data on neutrino-nuclear interactions to make determinations of how these interactions depend on interactions the size of the nucleus. So MINERvA will be able to predict what an Argon experiment like DUNE (Deep Underground Neutrino Experiment) [1] would be like. The energy of the neutrino beam also has an effect on these cross sections, which MINERvA also measures.

1.5 MINERvA Experiment

Neutrino interactions are so challenging to measure that we did not know how they interact with nuclei at the 20 percent level (before MINERvA). Oscillation experiments, if their data is to be well understood, it is useful to have a good grasp on how neutrinos interact with any detectors we could conceivably build. MINERvA is an experiment designed to do just that.

A neutrino beam is generated close to MINERvA's 170 tonne detector it plunges through 240 meters of solid rock before entering the detector. Once in the detector neutrinos encounter nuclei of five different materials, interact, and tracks are created from the energy deposited in the detector by the products of the interaction, "final state particles". Finally, we are able to reconstruct the interaction by turning those energy deposits into digital signals which can then be read by a computer and the trajectory of particles mapped with "tracks".

1.5.1 NuMI Beam: Creating the Neutrinos

Neutrinos at the Main Injector, or NuMI, is a project at Fermilab which creates an intense beam of neutrinos aimed towards the Soudan Mine for use by several oscillation and neutrino-nucleus particle detectors. As of June 2019, only NOvA experiment uses the NuMI beam. MINERvA ceased operation, on February 26, 2019, after ten years of taking data, and MINOS stopped June 29, 2016.

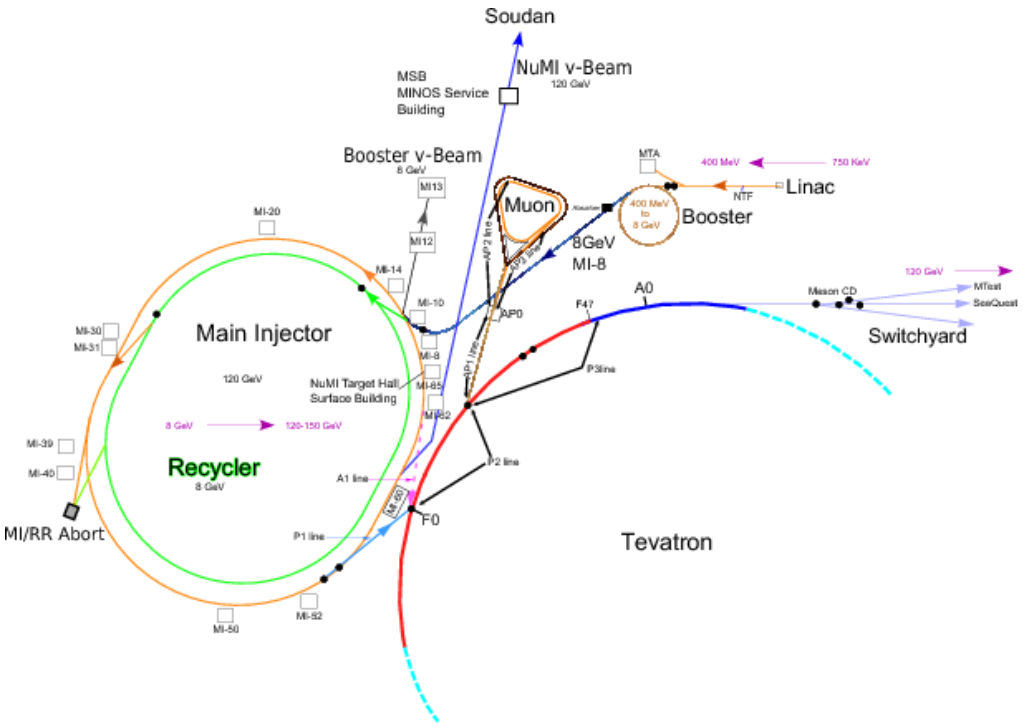

Figure 4: Schematic diagram of the complicated experimental setup at Fermilab, Batavia, Illinois. Neutrino beam begins with protons at the linear accelerator or Linac in upper right. [4]

Neutrino production

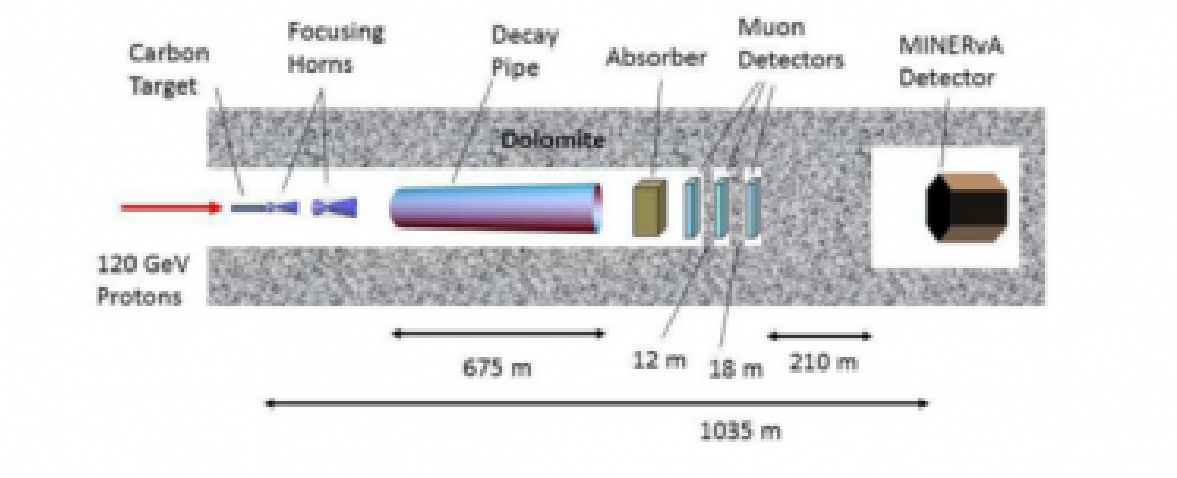

Figure 5: Schematic diagram of MINERvA detector, Fermi National Laboratory, Illinois. [20]

The proton beam begins the beam cycle in the Pre-Accelerator (Figure 4) which accelerates protons to 750 keV. Then the protons go to the linear accelerator, or LINAC, which gets the kinetic energy to 400 MeV and then the booster speeds it up to 8 GeV. After, they are poured out into the Main Injector which brings the energy up to 120 GeV.

The Main Injector is a system of electromagnets and microwave cavities that are used to accelerate the protons around the ring to store them until a spill happens. A "spill" is when the main injector dumps about 20 $\times 10^{12}$ protons into the NuMI beamline. The spills are 10 microseconds long and occur every 1.667 seconds.

The first step, shown in Figure 5 in the production of the NuMI beam is to direct a beam of protons from Fermilab's main injector onto a carbon (graphite) target. The proton beam interacts in the target to produce mesons, mostly pions and kaons, which are focused toward the beam axis by two magnetic horns, which function like convex lenses. The focusing horns can be set in two "modes" by changing the direction of the 185 kA current. When the horns focus positively charged pions and kaons the resulting beam is mostly neutrinos, and when focusing negatively charged pions and kaons the beam is mostly anti-neutrinos. Some contamination within both of the

beams from particles of the opposite type does occur. Positive mesons then decay into anti-muons and muon neutrinos while in the decay tunnel.

A hadron absorber downstream of the decay tunnel then removes the remaining protons and other hadrons from the beam. The muons are absorbed by a wall of rock. The neutrinos continue through to the MINERvA, MINOS, and NOvA near detectors on-site at Fermilab.

The neutrinos then travel through the earth to the MINOS far detector cavern in the Soudan Mine 735 km away from the NOvA far detector 810 km away at Ash River, MN, then onwards into space.Neutrinos interact so rarely in rock, that no beam tunnel is needed. Even a neutron star would be mostly transparent to neutrinos.

1.5.2 The MINERvA Detector

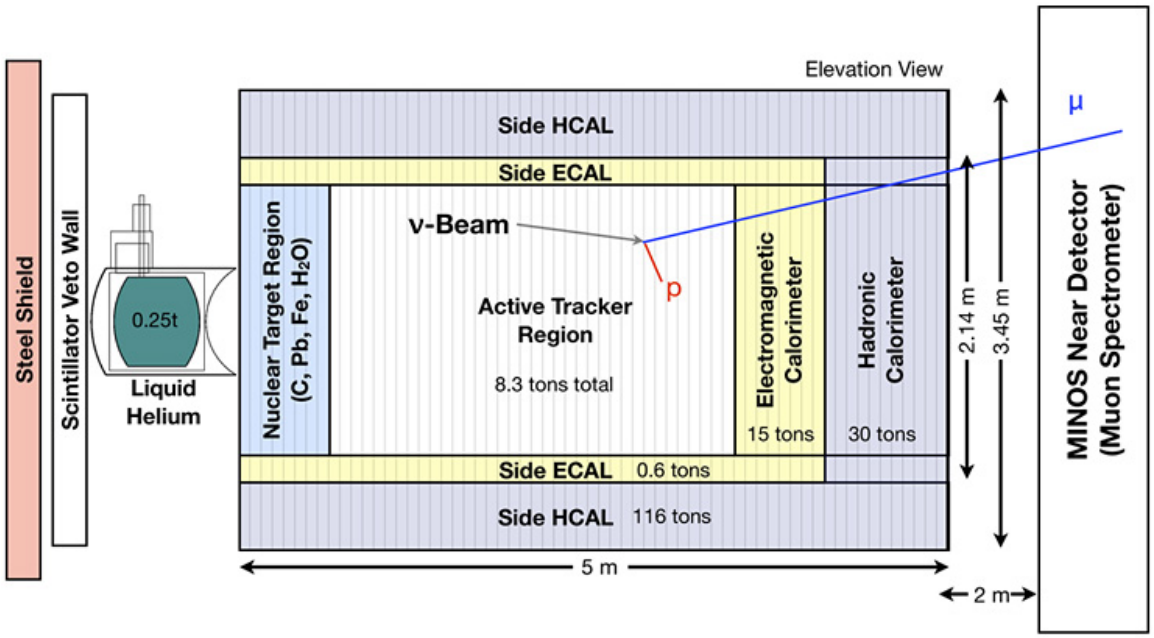

Figure 6: Schematic diagram of MINERvA detector: Fermi National Laboratory, Illinois: Inner Tracker Region, HCAL, ECAL, Nuclear Target. The proton and muon are tracked in the MINERvA detector. [5]

The MINERvA detector is positioned directly in the NuMI beam line at Fermilab where neutrinos and anti-neutrinos with peak energy at 3 GeV. It is convenient for the model only testing in this thesis to choose just one energy, so 3 GeV is used. The collaboration has a range of neutrino and anti-neutrino interactions to study.

The MINERvA experiment (Figure 6) has two main regions,the inner tracker region and an "upstream" nuclear target region. The inner tracker region is made up 120 hexagonal planes each 2.2 meters wide. Scintillator is polystyrene with pseudocuimene, a chemical that fluoresces when energy is deposited by a charged particle or high-energy photon. With carbons and hydrogens, scintillator serves as both the neutrino target and the detection medium comprises the bulk of the detector. The plastic scintillator planes are arranged in stacked sequences to allow for 3D reconstruction of events with especially good measurements of the particle's direction.

More tracking layers continue upstream of the inner tracker to the nuclear target region where layers of carbon, iron, and lead are scattered throughout. In addition, upstream from the solid target regions there is a helium target.

The detector also has an electromagnetic calorimeter, or ECAL, region which detects electrons, positrons, and photons by detecting their charged secondaries. These particles, usually photons and electrons with various energies race through layers of scintillator and 2 mm thick slices of lead. If photons have high energies they will travel a certain distance and produce an electron-positron pair or and give up half their energy to a photon in bremsstrahlung or electrons will. Less energetic secondary electrons may not even make it through the ECAL. This is the so-called electromagnetic shower.

Behind the ECAL is a hadron calorimeter, or HCAL, comprised of one inch steel plates between scintillator planes. As with the ECAL the HCAL is able to measure the energy and direction of the particle and does so by triggering the more complex hadronic particle shower. Both calorimeter regions along the sides of the detector are used to measure particles leaving the active region either scattered at large angles or coming off of the neutrino-target interaction point. [15]

Putting this together, if there is a charged muon and a proton coming from the interaction, they will be well measured. The muon and proton trajectories are marked "tracks". The particle tracks are assigned measured energies and momentum vectors

based on energy calibrations and their measured directions. As we will see, this allows us to learn quite a bit about that initial weak interaction inside a carbon nucleus.

1.6 Simulating Neutrino Events: GENIE

1.6.1 Models/Simulation as a Tool

Simulation is a tool used to model these events as if they had happened in a nucleus. There are a number of simulations used in the neutrino physics business. One of these is a collection of processes simulated called GENIE. [6]

From GENIE's manual, "GENIE is a collection of software and application products for the experimental neutrino physics community. This suite includes
i) a 'Generator' which is a collection of software to simulate various processes in the nucleus,
ii) massive archives of neutrino,charged-lepton and hadron scattering data and software to allow for data-Monte Carlo 'Comparisons', and
iii) a generator 'tuning' framework and data fitting applications . "

This thesis describes and fixes a flaw in one component of GENIE then explores how large an effect it has. GENIE begins generating an event according to cross-sections derived from past neutrino experiments. This open source software, which is the focus of this report, is maintained, improved, and used daily by thousands of neutrino physicists around the world. These physicists largely work on the largest neutrino-nucleus scattering and oscillation experiments like T2K, MINERvA, MiniBooNE, MicroBooNE, DUNE, and MINOS.

GENIE pulls the cross section for a particular reaction and its Monte Carlo algorithm generates events accordingly. The physics models used in GENIE incorporate many important scattering mechanisms ranging in energy from a few MeV to hundreds of GeV and are used to simulate any neutrino flavor and target type. These physics models can be placed into three groups: nuclear physics models, cross section models, and final state interaction (FSI) rescattering models.

1.6.2 Nuclear Physics Model

These are the models concerned with what is happening even before the neutrino gets there. This is crucial for determining the scattering kinematics in an event. This means considering the size of the nucleus, how tightly bound the nucleons are (a well

with negative potential energy), and what motion they have in the nucleus. The Fermi Gas models are included in this category. More will be said about this model later.

1.6.3 Cross Section Model

The cross section model allows for the calculation of the cross sections. The cross sections for neutrinos scattering off nuclei (coherent), nucleons (quasielastic), and quarks (deep inelastic scattering-DIS) are included here. During event generation the cross section is used to determine the distribution of the energies of interacting neutrinos. The cross sections for specific processes at each energy are then used to determine which interaction type will occur, and the distributions for that interaction model are used to determine the event kinematics. Cross sections can also be precalculated and stored for multiple uses speeding up computation time to determine muon and proton scattering angles, how many and what type of hadrons are knocked out of the nucleus.

1.6.4 Intranuclear Hadron Transport and FSI

GENIE includes models for final state reinteractions. These are reactions where the hadron created through initial neutrino interaction reinteracts with other nuclei before being leaving from the nucleus.These are strong force interactions resulting in additional single and mutlinucleon knockouts.

INTRANUKE is a subpackage in GENIE to model rescattering of pions and nucleons in the nucleus. The particles can collide with either one other nucleon or have no reinteraction before exiting the nucleus. Various FSI processes are modeled in INTRANUKE.

One particular process, elastic scattering, involves a hadron-nucleus coherent scatter. This process showed some peculiar properties when quantities of interest were plotted. This thesis examines the old and fixed elastic FSI code in INTRANUKE.

The version of GENIE being used here is 2.12.10. The bug is in the routine TwoBodyKinematics. It affects elastic scattering for all GENIE versions from 2.6 to 2.12 and for inelastic scattering into the GENIE 3.0 releases, though elastic scattering

was disabled in the latest simulation. The tests are done with the hA INTRANUKE FSI option, which is the default, but the problematic code is used by all FSI options.

1.6.5 GHEP Event Record

The GHEP Record is an output that prints to the screen all the simulated kinematic information about particles involved in an interaction. Each particle has a code number, its momenta and mass are printed for each event. Figure 7 below shows a special event GHEP record.

```
|----------------------------------------------------------------------------
|GENIE GHEP Event Record [print level:   3]
|----------------------------------------------------------------------------
| Idx |          Name | Ist |        PDG |   Mother  | Daughter  |      Px |      Py
|----------------------------------------------------------------------------
|   0 |         nu_mu |   0 |         14 |  -1 |  -1 |   4 |   4 |   0.000 |   0.000
|   1 |           C12 |   0 | 1000060120 |  -1 |  -1 |   2 |   3 |   0.000 |   0.000
|   2 |       neutron |  11 |       2112 |   1 |  -1 |   5 |   5 |  -0.034 |  -0.045
|   3 |           C11 |   2 | 1000060110 |   1 |  -1 |   7 |   7 |   0.034 |   0.045
|   4 |           mu- |   1 |         13 |   0 |  -1 |  -1 |  -1 |   0.197 |   0.553
76)
|   5 |        proton |  14 |       2212 |   2 |  -1 |   6 |   6 |  -0.232 |  -0.597
|   6 |        proton |   1 |       2212 |   5 |  -1 |  -1 |  -1 |   0.000 |  -0.549
|   7 |      HadrBlob |  15 | 2000000002 |   3 |  -1 |  -1 |  -1 |   0.000 |  -0.597
|   8 |      NucBindE |   1 | 2000000101 |  -1 |  -1 |  -1 |  -1 |   0.000 |  -0.048
|----------------------------------------------------------------------------
|       Fin-Init:                                                |   0.197 |  -0.642
|----------------------------------------------------------------------------
|       Vertex:          nu_mu @ (x =     0.00000 m, y =     0.00000 m, z =     0.000
|----------------------------------------------------------------------------
| Err flag [bits:15->0] : 0000000000000000    |  1st set:
| Err mask [bits:15->0] : 1111111111111111    |  Is unphysical:    NO |   Accepted:
|----------------------------------------------------------------------------
| sig(Ev) =       5.49567e-38 cm^2  | dsig(Q2;E)/dQ2 =          8.20697e-39 cm^2/GeV^
|----------------------------------------------------------------------------

----------------------------------------------------------------------------
GENIE Interaction Summary
----------------------------------------------------------------------------
[-] [Init-State]
 |--> probe        : PDG-code = 14 (nu_mu)
 |--> nucl. target : Z = 6, A = 12, PDG-Code = 1000060120 (C12)
 |--> hit nucleon  : PDC-Code = 2112 (neutron)
 |--> hit quark    : no set
 |--> probe 4P     : (E =     3.000000, Px =     0.000000, Py =     0.000000, Pz =
 |--> target 4P    : (E =    11.174863, Px =     0.000000, Py =     0.000000, Pz =
 |--> nucleon 4P   : (E =     0.919976, Px =    -0.034429, Py =    -0.044553, Pz =
:
```

Figure 7: Screenshot of the GHEP Record Information included are momenta for all particles, particle identification codes and names, particle masses, momentum transfer information, hadron invariant mass.

In Figure 7 Index Idx 0 (muon neutrino) strikes Idx 1 (^{12}C nucleus-at rest) producing Idx 2 (neutron), Idx 4 (muon), and Idx 4 (^{11}C nucleus) plus Idx 5 (a proton). Then in this specific elastic scatter, the proton reinteracts with Idx 3 to produce Idx 6, the final state proton. Of course Idx 3 has daughter particle the remnant nucleus labeled Hadrblob and Idx 5 has as its daughter particle Idx 6. The four-momentum of each particle is also shown at each step.

1.7 Relativistic Kinematics

Relativistic kinematics is the physics of motion for particles moving near the speed of light. There is a standard problem in relativity of an event occurring in one reference frame, and an observer witnessing such an event from another reference frame. For the two-body reactions in this thesis, the observer is in the "lab" frame. The reaction event is best described in the two particle center of momentum frame (CM). In the CM frame the two particles are necessarily travelling back-to-back with equal momenta, but could have different energies and masses. This must be true before and after the scattering in order to conserve zero net momentum.

There are two postulates of special relativity. The first says that whether that frame is at rest or moving at a constant speed an observer in either frame is unable to tell the difference even after measuring physical quantities. The second maintains that the speed of light, c, is the same in all frames of reference. As a consequence, transforming events between reference frames is not as simple as in introductory physics.

1.7.1 Frames of Reference

Consider two inertial (non-accelerating) reference frames O and O' as shown in Figure 8. Their x-axes coincide at time t=0s. O remains at rest while O' moves along the x-axis with a speed v with respect to O. An event e occurs at time t=t_e. An observer in rest frame O experiences the event in differently than an observer in O'. Figure 8 shows such a setup.

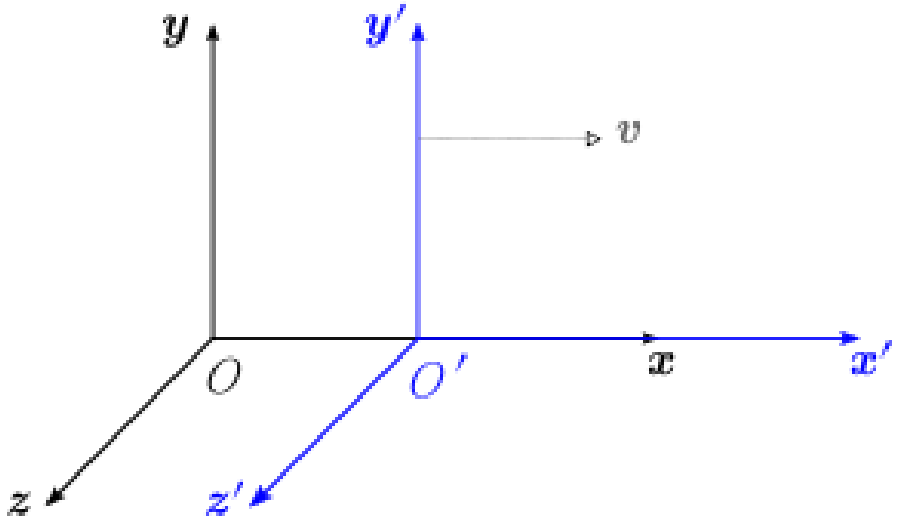

Figure 8: Two inertial reference frames are placed side by side. O' moves at a constant speed while the other, O, remains at rest. Diagram from [12]

1.7.2 Four Momentum and Lorentz Transformations

We define the four momentum of a particle to be a 4 component vector. The four-vector is a space-time location for any event. The space-time point

$$(x_0, x_1, x_2, x_3) = (ct, x, y, z) \tag{6}$$

is the event's location in O. The event's location in O' is

$$(ct', x', y', z') = (x'_0, x'_1, x'_2, x'_3) \tag{7}$$

The four momentum is a four vector comprised of a particle's energy and momentum.

$$(\frac{E}{c}, p_x, p_y, p_z) \tag{8}$$

A particle's energy is not simply due to its momentum. It also has energy due to its mass.

$$E^2 = P^2c^2 + (mc^2)^2 \tag{9}$$

where E is the particle's energy, P the magnitude of momentum, and m its rest mass. If the particle is at rest, we obtain Einstein's famous observation that mass is a form of energy.

Constructing these frames changes as you move closer to the speed of light. Next we explore the method employed in special relativity, the Lorentz boost. This will prove useful in our hadron-nucleus scatter experiments where center of momentum frame is often used to report findings.

The Lorentz transformations are a set of equations that transform the observer from one frame to another. In this thesis transformations to the special center of momentum (also called center of mass) frame are used. These transformations are succinctly described in the simplest cases by a kind of rotation matrix. All four-vectors will transform in this way under a Lorentz transformation.

A "boost" from one frame to another allows an observer to determine the space-time coordinates or the energy and momentum four-vector of an event in the other frame. The "boosted" frame can be considered the frame in motion. However, according to the tenets of special relativity it is impossible to tell,as an observer, which frame is the boosted one. As such, it is enough to know the relative speed of one frame with respect to the other. This speed is often called the boost and is represented by the Greek symbol $\vec{\beta} \equiv \vec{v}/c$. By dividing the speed v by the speed of light c, β is a unitless quantity. We also define another useful related quantity $\gamma \equiv \frac{1}{\sqrt{1-\beta^2}}$

$$t' = \gamma\left(t - \frac{vx}{c^2}\right) \tag{10}$$

$$x' = \gamma\left(x - vt\right) \tag{11}$$

$$y' = y \tag{12}$$

$$z' = z \tag{13}$$

Lorentz Boost in the x direction $\beta \equiv v/c$, $\gamma \equiv \frac{1}{\sqrt{1-\beta^2}}$ Note that the x component is the only component of the three momentum that is translated in time.

The γ factor is what makes these equations particular to special relativity. Observers in different reference frames (lab or CM) measure different values for the time, location, energy, and momentum of the same particles. γ lets us know how close the system's motion is to the speed of light and allows us to transform coordinates accordingly.

1.7.3 Conservation Laws

The total four momentum is conserved in any interaction. In every reference frame, this means that both energy and momentum are conserved separately. The dot product of two four vectors

$$(E_a, \mathbf{a}) \cdot (E_b, \mathbf{b}) = E_a E_b - a_x b_x - a_y b_y - a_z b_z \tag{14}$$

is invariant under a Lorentz transformation. Lorentz-invariant quantities are key in kinematics calculations for all manner of experiments.

In particular a four-momentum of a particle with itself becomes E^2 - p^2c^2 which is the square of the particle's rest mass energy, $(mc^2)^2$, see Equation 9.

2 The QE Sample and Transverse Kinematic Variables

2.1 QuasiElastic Neutrino Interactions

The Quasielastic (QE) neutrino event is a neutrino interaction in which the neutrino hits a nucleon in a billiard ball type of scattering. The neutrino exchanges a W boson in a charged current reaction with that nucleon to produce a new hadron and a new lepton. The scattering can also be interpreted as the muon neutrino emitting a virtual W. The W carries with it the weak force, which transfers momentum and charge to the neutron turning it into a proton. However, unlike elastic billiard ball scattering, kinetic energy is not perfectly conserved. Some kinetic energy is used to remove the nucleon from the nucleus, more is turned into the mass of the muon. So this type of interaction is called quasi elastic.

The QE sample is one the most important parts of the MINERvA sample. The MINERvA analyses and this study are focused on the charged current reactions because we can measure both outgoing particles. Here we are particularly focused on events where a muon μ and a proton are in the final state. Hadrons in the final state that result from the neutrino interacting with a single nucleus must exit that nucleus to be sensed in the detector. The muons are also easily tracked. Both of these particles are detected on MINERvA with good resolution. These events, as simulated in GENIE, form the subject of the bulk of the analysis here.

The scattering can also be interpreted as the muon neutrino emitting a virtual W particle which transfers momentum and charge to the neutron turning it into a proton. Figure 9 shows the Feynman diagram representation of this process, like 3. The W emission is the weak force in action. Wave-particle duality of nature allows us to say that the neutron's interaction with the field of the emitted W is the actual collision.

After the proton is created it has to travel somewhat in the nucleus before being ejected from the nucleus and detected. Here we use a model of the nucleus where nucleons are semi-free. The nucleons to have some momentum within the nucleus and momentum states are filled. It costs an average of 25 MeV to remove a nucleon

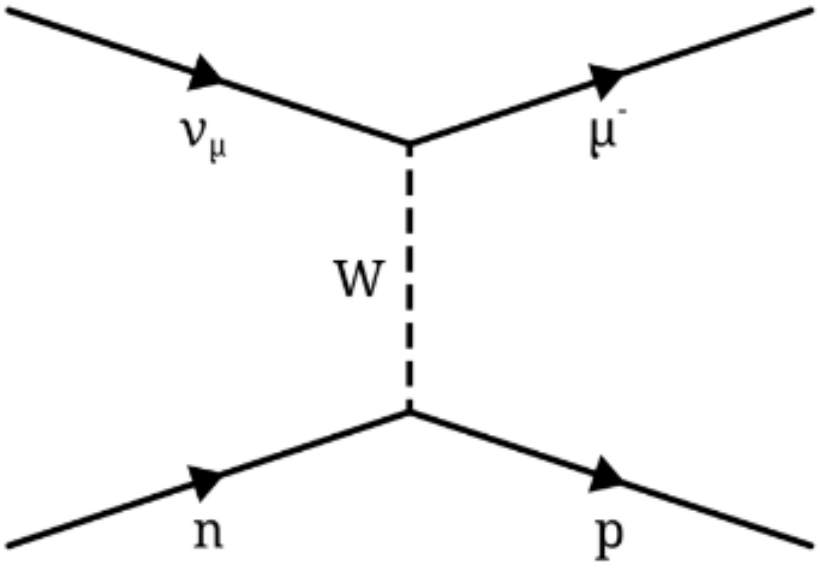

Figure 9: Feynman diagram for a quasielastic event. The muon neutrino scatters off of a neutron, exchanging momenta with the neutron and turning it into a proton while the muon neutrino becomes a muon. Diagram from [19].

from the nucleus.

The secondary reinteraction - proton colliding with a nucleon is also similar to a classical billiard ball scatter. When the neutrino scatters off a W it imparts momentum to the neutron in the process and then again from that newly created proton to another nucleon in a subsequent collision. Of course, during this process the energy and momentum of all particles is conserved. This means that in both lab and center of momentum frames energy and momentum are both conserved separately.

2.2 Fermi Motion

A spectral function is one that models the momentum states of nucleons and takes into account the energy required to remove that nucleon. There are a few models for the distribution of momentum states within the nucleus.

Fermi motion is the natural quantum mechanical motion of particles bound to the nucleus. Nucleons, because they are fermions, are required to individually occupy a different single-particle state. In the limit that interactions can be ignored, the ground state of a nucleus is one with nucleons filling up all the single-particle states in order of their energies, starting from the lowest one.

The Fermi gas model is a theoretical concept applied to particles weakly interacting, as in an ideal gas. In this model, nucleons separately fill up momentum states uniformly until the Fermi energy E_F is reached. The result is a distribution characterized by a sphere in momentum space. The radius is the Fermi momentum. Beyond this point ($\sim$ .226 GeV/c for Carbon) states are not occupied. This produces a sharp "cliff" feature shown below in Figure 10. Beyond this region, an extension by

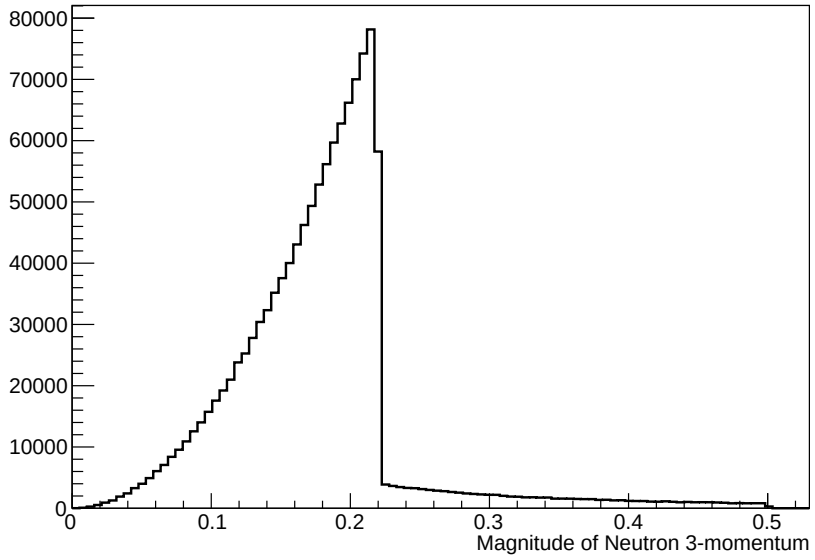

Figure 10: GENIE's actual distrbution of neutron momenta. The Bodek-Ritchie tail results from nucleon-nucleon correlations not ordinarily included in final state interaction mechanisms.

Bodek and Ritchie [9] accounts for some population of states beyond the Fermi radius. This happens because Bodek-Ritchie takes into account processes where two nucleons could be in a correlated state with extra momentum. It is used as a replacement for a spectral function.

Other models like the Benhar-Fantoni spectral function are a two-dimensional distribution of momentum and removal energy. Some spectral functions are plotted in Figure 11. It is the black line to be compared with the green line like 10. The Bodek-Ritchie tail in Figure 10 attempts to provide mucleons beyond the Fermi Energy. MINERvA expects to use data to distinguish these two by measuring the neutron momentum P_n for QE events. All show some sort of sharp decrease in probability between 0.2 and 0.3 GeV.

There is an energy cost to the particle removed breaking free of the strong interactions holding it in the nucleus. Some nucleons are more difficult to bring out than others. In GENIE the removal energy is set to 25 MeV for all nucleons. We expect the resulting ^{11}C nucleus is also in an excited state.

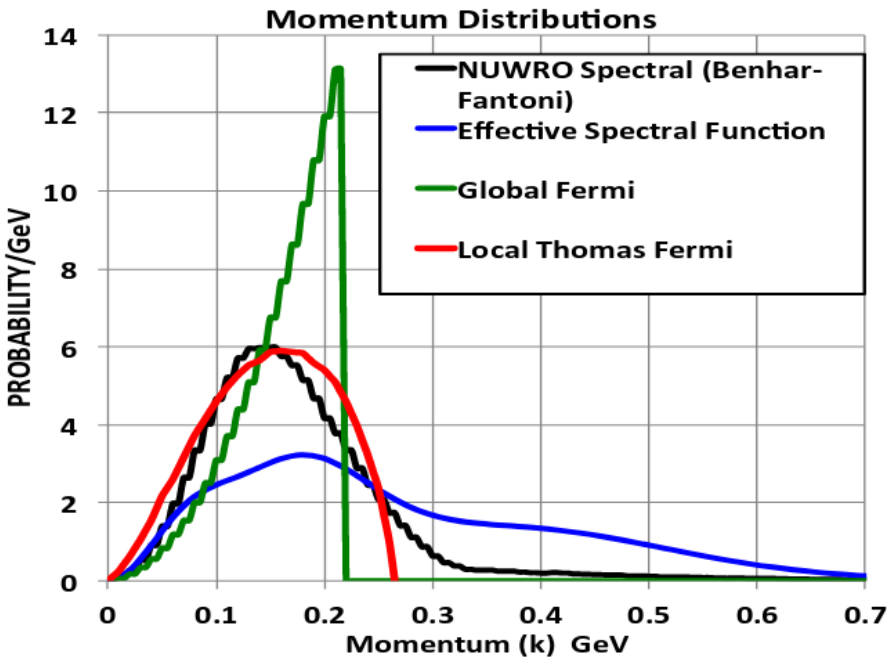

Figure 11: Spectral Function (black)is shown along with Fermi gas (Green). Ignore the blue curve. Taken from [8].

2.3 Final State Interactions

The initial proton then reinteracts with other nucleons or the nucleus as a whole. These reinteractions on final state particles are often referred to as final state interactions, or FSI. More than half of the protons from a QE event will participate in reinteraction in carbon. It is important to develop models to describe FSI better and also to understand the models' limitations because FSI contributes significantly to the systematic errors in neutrino oscillation measurements. MC codes used in major neutrino oscillation experiments (FLUKA, NUANCE, NEUT, GENIE) in their description of FSI effects use the model of intra-nuclear cascade (INC).

In this model the outgoing proton is assigned mean-free distance to interact with nucleons. It is a semi-classical approach in which some quantum effects can also be incorporated. Theoretical arguments for the applicability of the cascade model began nearly a half century ago[14]. In the INC models, the hadron sees a single nucleon. The probability of interaction with that nucleon is given by the cross section for that interaction and the density of nucleons. The specific outcomes of FSI is then chosen based on measured cross sections for those outcomes.

GENIE simulates various different FSI processes. These outcomes, or "fates" allow for multiple different possibilities of nucleon-nucleus interactions. The fates discussed here will be the charge exchange, elastic scattering, inelastic scattering, multinucleon knockout, and pion production.

Figure 12 summarises the FSI fates and their fraction of the total events generated in the final state. The white is no-FSI events, the blue color is elastic, the orange is inelastic, and the red is multinucleon knockout. Pion production accounts for such a small number of events we will not pay much more attention to it here. This color scheme is used throughout this thesis.

Note that the no-FSI events make up the bulk of the sample followed by elastic scattering. The ratio of elastic events to no-FSI events is about 0.48. This report focuses specifically on the elastic scattering process simulation in GENIE.

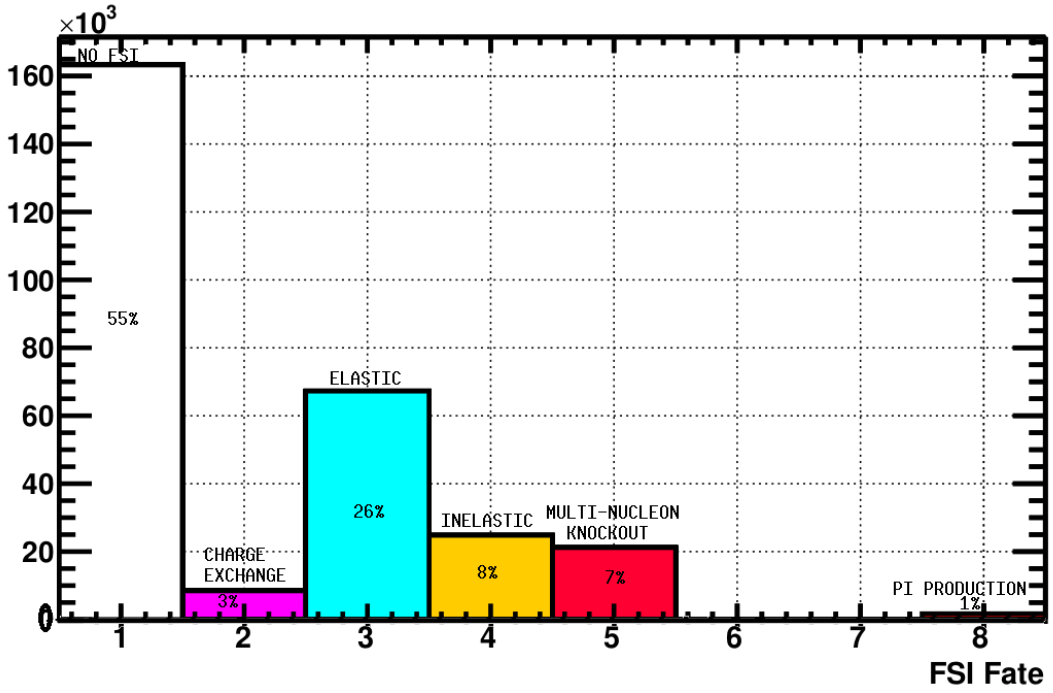

Figure 12: All FSI processes and percentage of total processes

Neutrino interaction experiments like MINERvA provide a lot of information on final state particle content. We observe that a model for FSI is always needed. However, the specific mix of outcomes is uncertain and has been difficult to constrain. What we use comes primarily from separate hadron-nucleus scattering experiments.

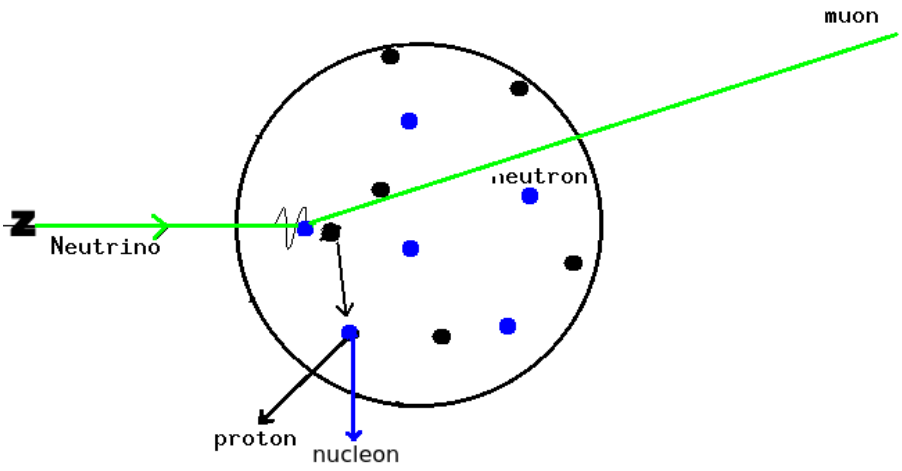

Figure 13: Inelastic scattering final state interaction, the proton kicks out another nucleon

Inelastic scattering (Figure 13) is the process by which that the proton collides with another nucleon and both exit the nucleus. The final state particles are the proton (with transferred momentum from the neutrino to the struck neutron) and another nucleon kicked out after being hit by the proton. The other nucleon could be either a proton or a neutron. The result is either a $^{10}C^{*}$ nucleus or $^{10}B^{*}$ nucleus, most likely in an excited state.

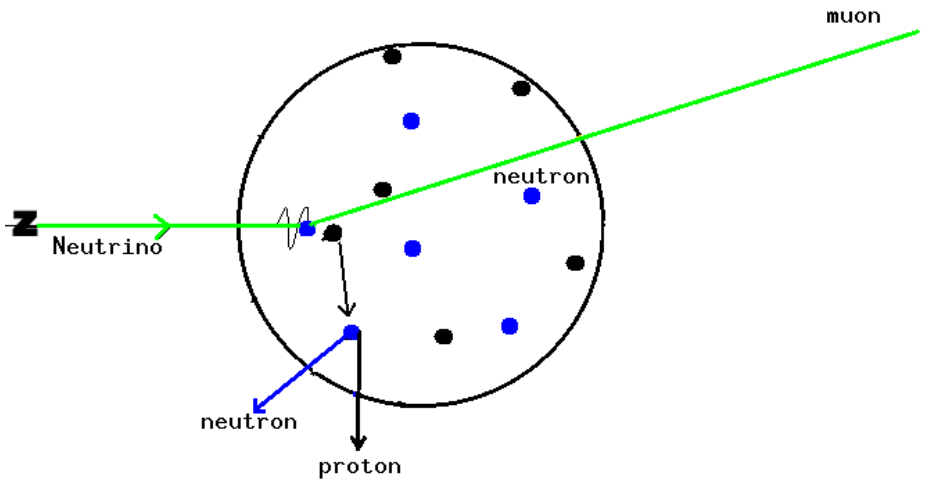

Figure 14: Final state charge exchange fate, proton and neutron exit the nucleus right after the quark exchange also swaps their charges.

Figure 14 shows the charge exchange process. In it, the final state proton exits with a neutron and they exchange charges via a charged pion. The particles left over in the final state are still a neutrino, a proton, another nucleon, and an excited Carbon-10 nucleus. A Feynman diagram of this would show the neutron releasing a down quark while the proton accepts it and releases an up quark.

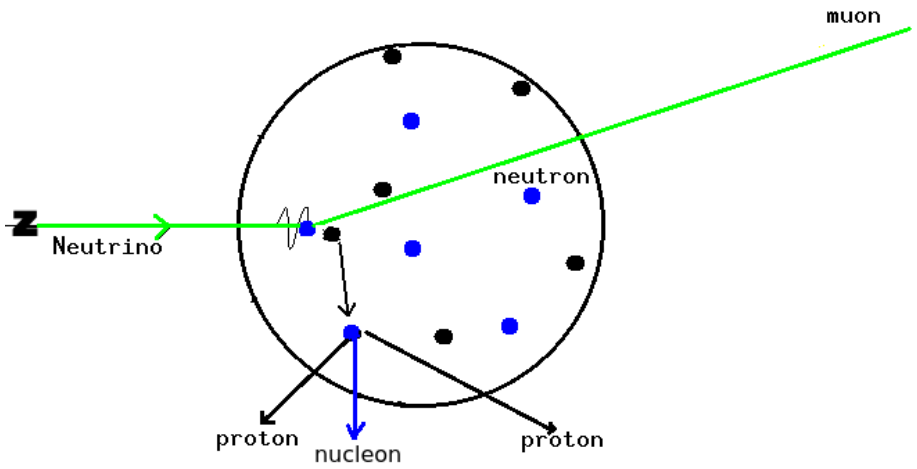

Figure 15: Many particles may exit the nucleus following collision

Multiparticle knockout is the a proton colliding with another multiple nucleons, so many particles exit the nucleus in the final state. We expect these nucleons to share the total kinetic energy. This diagram (Figure 15) shows an interaction on a quasi-deuteron (neutron-proton pair) breaking it up and knocking both out as well. In GENIE's FSI model this also accounts for multiple scattering of nucleons as they exit.

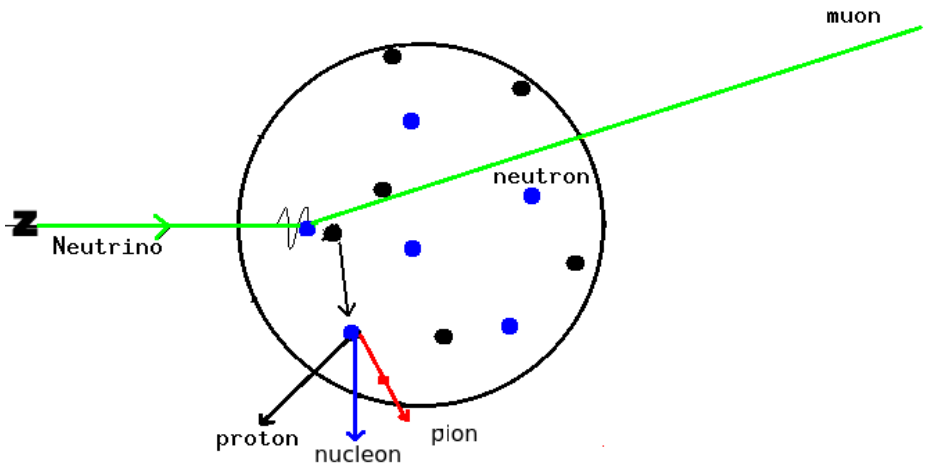

Figure 16: A proton and another nucleon exit the nucleus along with one pion, usually a π^+ less often a π^0.

Pi Production (Figure 16) is the only way a QE process that can have pions in the final state. This is also a multiparticle knockout process. Usually two nucleons exit after collision along with a pion and leave an excited nucleus.

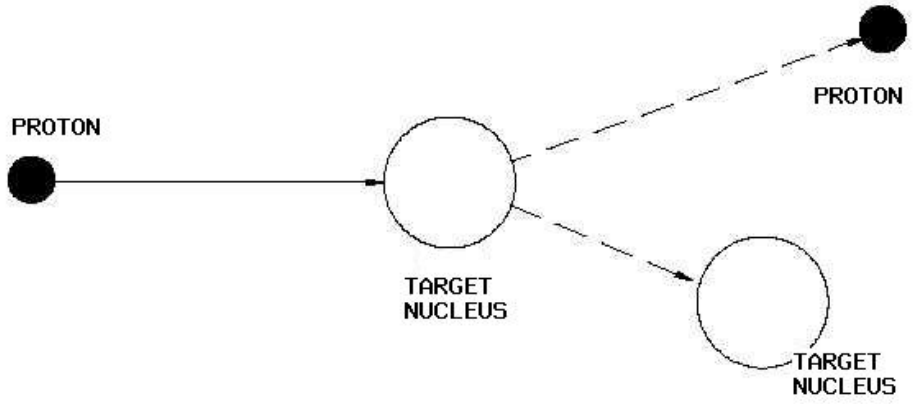

Figure 17: Elastic final state interaction- proton scatters off of ^{11}C nucleus

Elastic scattering, shown in Figure 17, is the process through which a proton scatters off of a nucleus. The proton and an excited carbon-11 nucleus are the only particles in the final state. Fixing GENIE's errors in simulating this process is the subject of this thesis. In the next chapter the solution is tested. In the fourth chapter, the results are analyzed.

Oddly enough this is an interaction with the nucleus as a whole, not just one of its constituent parts. But it is not so odd, the previous interactions are with nucleons, not their constituent quarks. And even billiard balls are not modeled at the single-atom level.

2.4 Transverse Kinematic Quantities

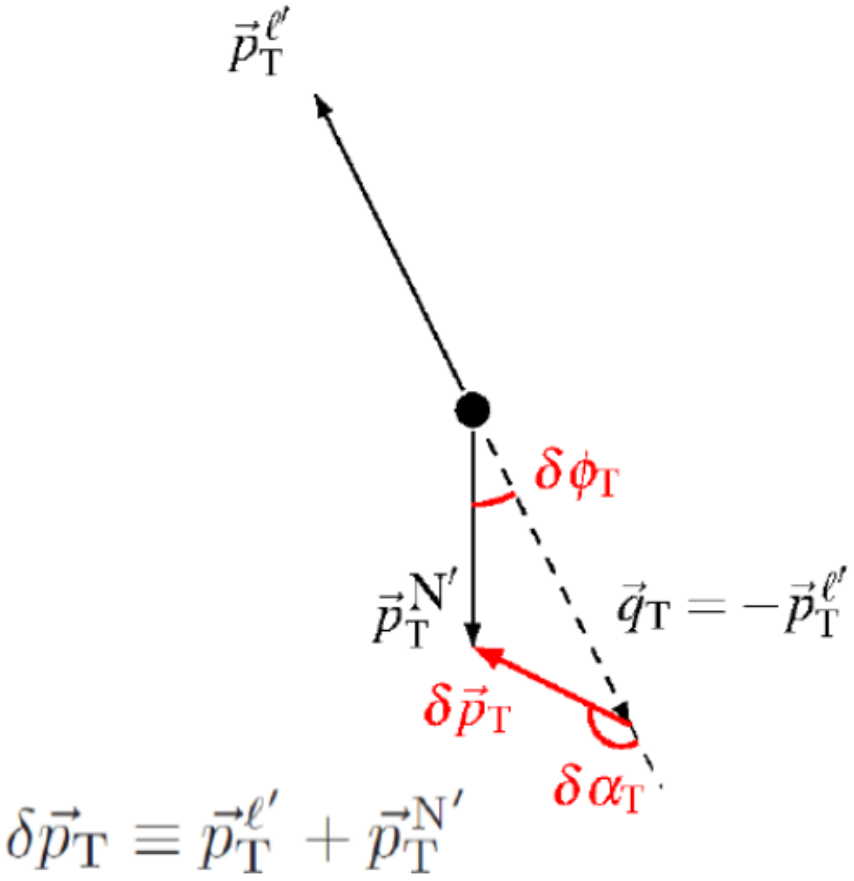

Figure 18: Diagram of Transverse Variables $\delta\phi_T$ Coplanarity, δp_T, $\delta\alpha_T$, p_n [16]

There are four variables (Figure 18) we create in the transverse plane, the plane perpendicular to the incident lepton. All of these can be computed from the measured four-vector energy and momenta of the muon and proton. The transverse kinematic variable distributions were separated by FSI fate. Our first clue that something might be amiss with the elastic portion of the FSI model was seeing the features that that particular mode of FSI produced in these distributions.

If there was no Fermi motion or FSI as in the case of scattering off of a free nucleon, the resulting proton would have exactly the same momentum vector the

neutrino lost. To conserve momentum the transverse component $p_{T_{proton}} = -p_{T_{muon}}$ so both particles must be back to back in the transverse plane. Coplanarity angle, $\delta\phi_T$ is zero in this case and there is no missing transverse momentum δP_T. Obviously then the Accelerating angle, $\delta\alpha_T$, would also be zero. Our interest is to model the imbalance or how they take on non-zero values due to Fermi motion and final state interactions.

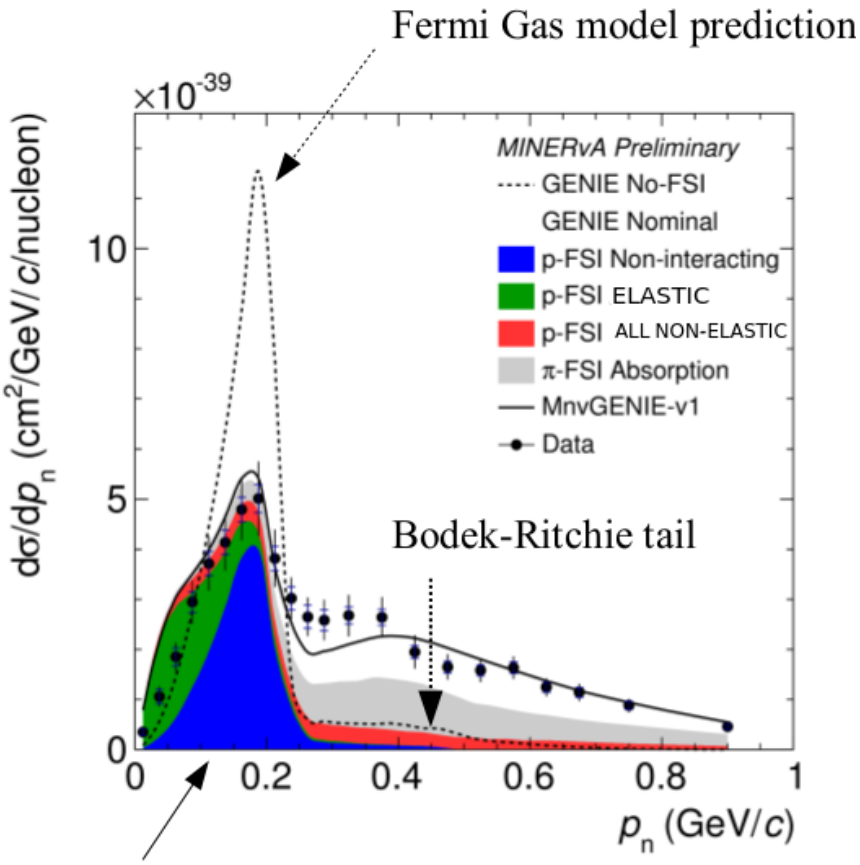

Figure 19: Published distribution P_n of mostly QE events, blue is FSI events generated without reinteraction occurring, red- non-elastic events, green- elastic events, dotted line represents GENIE configuration where no FSI events generated at all. [17]

Figure 19 is a plot of the fourth transverse variable p_n. It is the inferred neutron momentum of the neutron before the exchange of W with the neutrino. Data from the MINERvA experiment is also plotted. The QE portion makes up the bulk of the sample, but two other processes are also present. However, this report will focus only on the QE portion.

By neutrino standards, the model describes the data well almost everywhere. The model is within or just beyond the error bars on the data. However, the first four points before the peak are not well described because there is a mistake in the elastic FSI portion of the model.

2.4.1 Coplanarity $\delta\phi_T$

Coplanarity, as its name suggests, is a measure of how much out of the muon-neutrino plane the ejected proton's final momentum. This is a simple quantity to calculate and provides clues about transverse momentum picked up from Fermi motion. Protons in quasielastic interactions tend to be more in the plane than out.

If the coplanarity angle is zero degrees then there is no Fermi motion and no FSI happening. Since the neutrino comes from only the z direction the proton gets any transverse momentum from the neutron's Fermi motion. Then it may also pick up transverse momentum on reinteraction with other nucleons. In Figure 20 the white portion is the no-FSI model and deviations from zero are therefore due only to Fermi motion. The other fates show the combined effects of Fermi motion and that particular type of FSI and they are spread widely in coplanarity. The yellow portion is inelastic events, the magenta hadron knockout.

The elastic piece in blue appears to be even more coplanar than the rest of the sample as if the distribution were small angle smearing about zero. We expect the distribution to reflect a smearing due to Fermi motion. The preferentially coplanar elastic piece was clearly unphysical. The protons in the elastic portion should have at least had momentum transferred due to Fermi motion just as in the no FSI case.

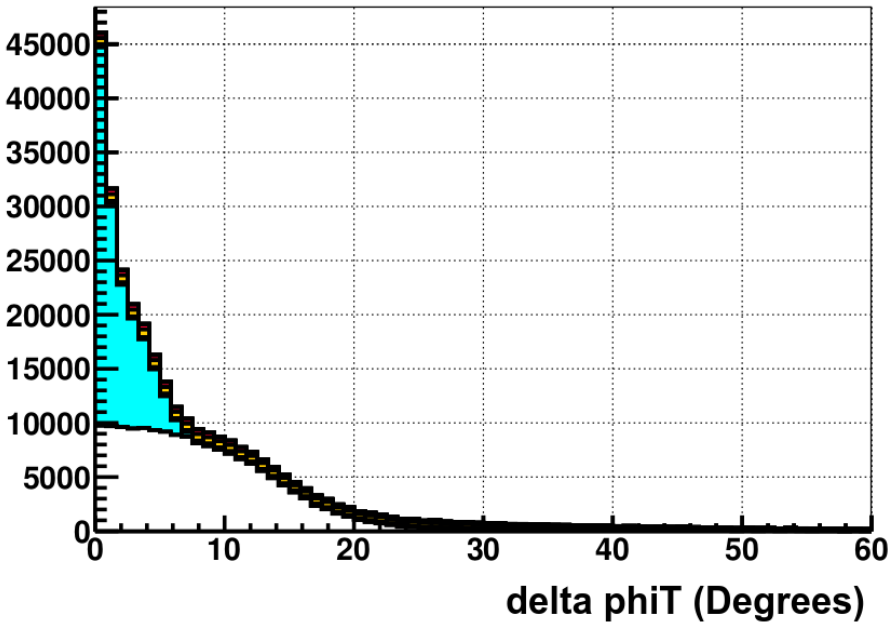

Figure 20: Coplanarity Angle distribution: blue-elastic, white-no FSI, red-inelastic, yellow-charge exchange, magenta-mutli-nucleon knockout. Note that the elastic piece is even more coplanar than the no FSI piece.

2.4.2 Transverse Momentum Imbalance δp_T

Transverse momentum imbalance in Figure 21 measures the magnitude of the vector difference in transverse momenta of the proton and projected transverse momenta of the muon. We expect in the limit of no Fermi motion and no FSI that the missing transverse momentum would be zero. Instead typical transverse momenta are 100 MeV, consistent with a large fraction of the original neutron Fermi motion. The blue elastic piece shows peculiar behavior in that it seems to peak at lower values than the no FSI component. We expect spreading around the Fermi motion peak (white) due to random small angle scatters.

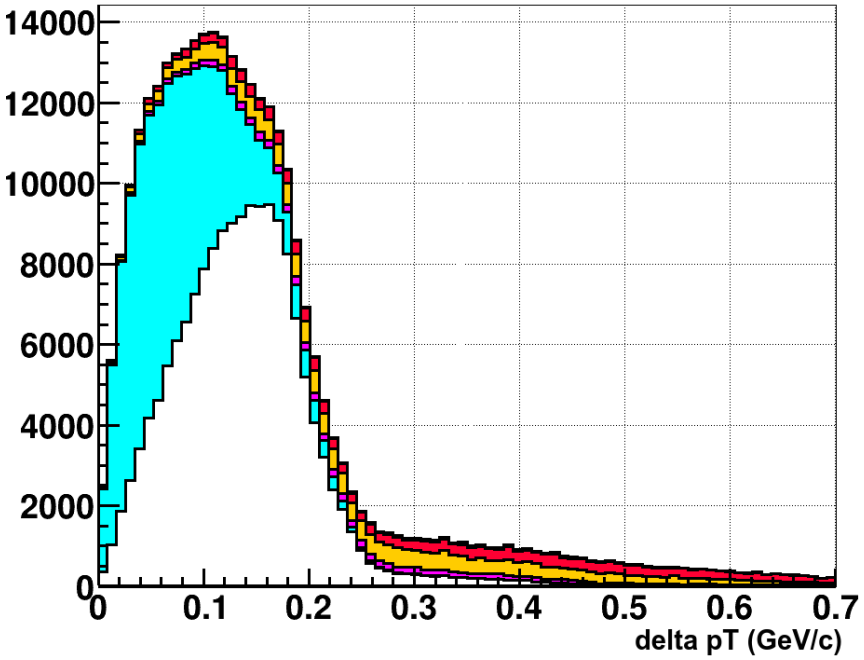

Figure 21: Transverse momentum imbalance δP_T is shown. Elastic events have even lower transverse momentum than the no FSI portion.

2.4.3 Acceleration Angle $\delta\alpha_T$

Alpha transverse measures the angle between the projected muon transverse,p_T^μ momentum and the momentum transfer vector $\delta\vec{p_T}$. When it is obtuse there is a large difference between the projected muon transverse momentum and the proton's transverse momentum. By definition, $\delta p_{Tproton}$ was smaller than expected and seemed to lose some energy. If $\delta\alpha_T$ is an acute angle implies that our proton probably gained some energy as it left the nucleus. Fermi motion only (white) can give either effect. FSI almost always leads to a real loss of energy given to knock out other nucleons.

In Figure 22 the white portion of the distribution has very little structure to it. The blue elastic on the other hand is running away at small and large angles.

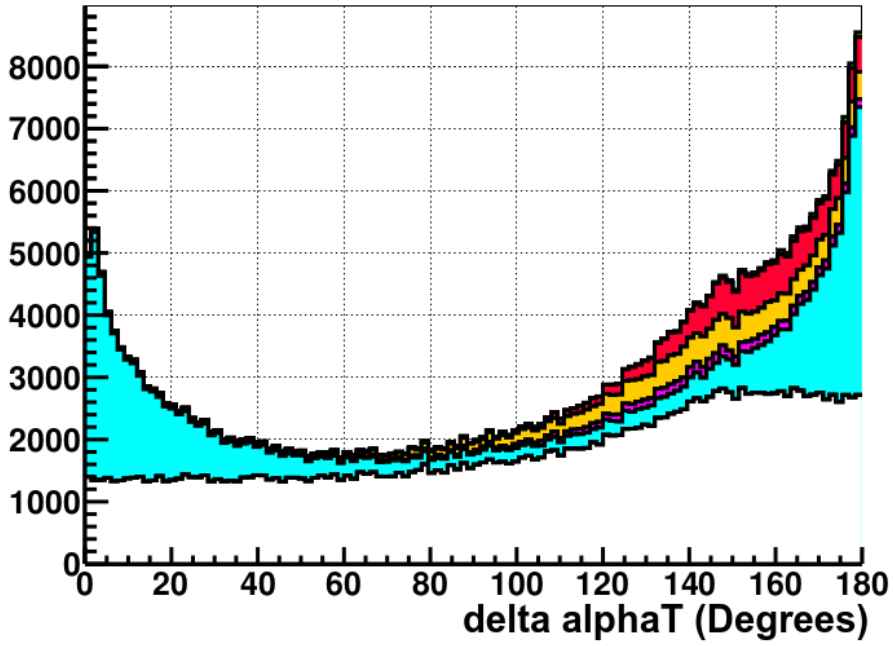

Figure 22: Figure above shows "Accelerating" angle $\delta\alpha_T$ distribution. The elastic piece shows unique features at small angles.

2.4.4 Inferred Neutron Momentum P_n

Since the transverse variables are especially sensitive to information about directionality and magnitude of momentum transfer as well as original Fermi motion it is possible to infer the original struck neutron's momentum even more precisely. Combining information about the transverse momentum of both proton and muon with longitudinal momentum transfer gives an estimate of the struck neutron's momentum. $p_n = \left|\vec{\delta}_{pT} + \vec{\delta}_{pL}\right|$. When there is no Fermi motion P_n would look exactly like the longitudinal momentum transferred to the system only. With Fermi motion, it should look like the neutron distribution supplied by GENIE.

Looking at Figures 23 and 19 with data, this mistaken elastic component is the barrier to seeeing how GENIE's Fermi motion is like nature's. Figure 23 shows a preferentially lower momentum for neutrons in an elastic scatter than those with just due to Fermi motion. Physically, this should not be possible because it would mean that after colliding with a nucleon, the proton on average had lost momentum nearly every time.

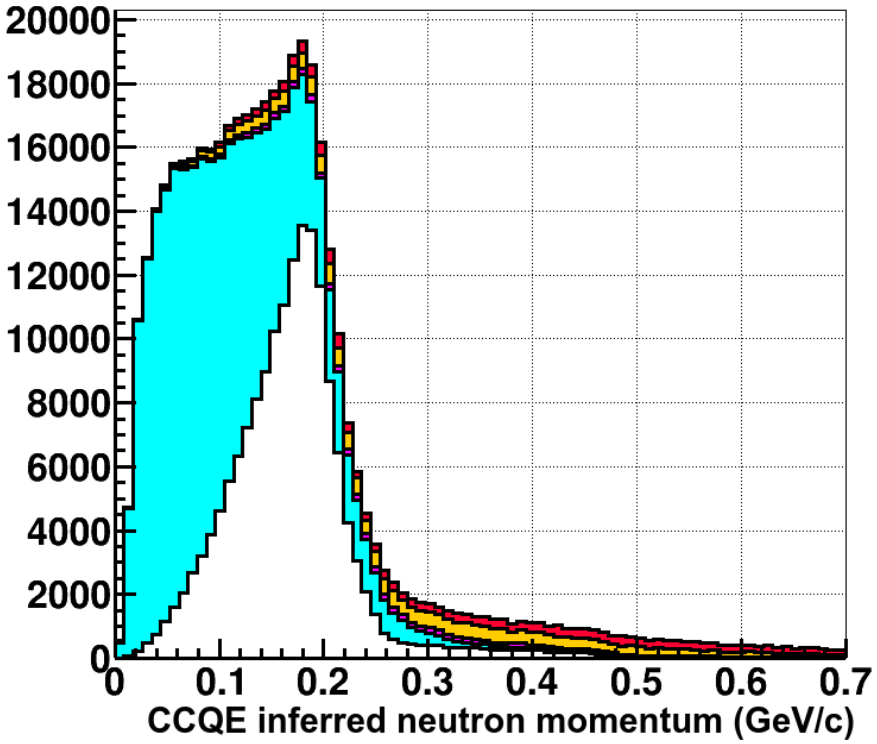

Figure 23: Calculated δP_T inferred struck neutron momentum. The elastic events are concentrated at a lower momentum than the no FSI events.

2.5 Acceleration

The spike at $\delta\alpha_T$ indicates these elastic scattered events correspond to acceleration of the proton. Figure 24 shows the change in kinetic energy that results from the scatter. Nearly all events show acceleration, though it is only 2 MeV which is a relatively small amount.

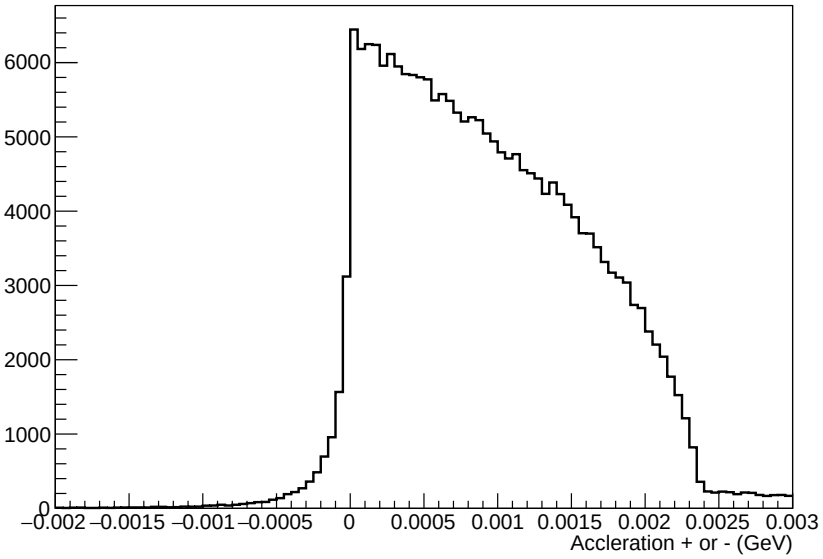

Figure 24: Change in proton kinetic energy after FSI collision. These elastic events are created with old code implementation.

3 Scattering

The elastic FSI scattering process is computed using a proton colliding with a Carbon-11 nucleus. For such a process, lab angle measurements such as proton angle with respect to the beam each correspond to a different center of momentum angle θ_{cm}. These are taken from deuterium experiments in the 70 s.[7]

We sample these θ_{cm} angles from an experimentally measured distribution. During the 1960s and 1970's nuclear physicists were interested in scattering experiments where particles like electrons, various hadrons, and positively charged particle beams were deflected by elastic collisions with atomic nuclei. These experiments were very popular because they shed light on the structure of nuclei, yielding important information about the scattered particle, and the forces between them.

One particular experiment, conducted at the LAMPF facility at Los Alamos National Laboratory in 1979, made an 800 MeV proton beam hit a target of oxygen-16 nuclei. Assuming the target nuclei are at rest, every measured lab frame angle is converted to θ_{cm}. Measurements of the rate were made at various proton center of momentum scatter angles are plotted in Figure 25 from the results published November 1979. [3]

Most scatters are at very small angles. Note that the vertical axis in Figure 25 is a logarithmic scale indicating that smaller angles are one thousand to ten thousand times more likely than larger. That y-axis is a cross section measurement showing, for an event, the likelihood of measuring a certain corresponding value of the proton's θ_{cm}. The distribution of CM scattering angles is used to approximate all elastic scattering final state interactions in GENIE.

The mechanism for scattering protons from the interaction can be treated as light passed around a central perfectly absorbing obstruction. The diffraction profile around the collection aperture produces the well known Airy pattern. For this reason the model in Figure 25 is called an optical model. It had parameters that were fit to these data.

It is unclear whether this is an entirely appropriate model for the elastic scattering which appears in the quasi elastic portion of the neutrino interaction sample. GENIE performs scattering of a proton already inside the nucleus rather than protons from

a beam, as in the experiment. Another inconsistency comes from the difference in the actual nuclear target used;the experiment uses oxygen-16 while we simulate on an excited Carbon-11 nucleus. GENIE also uses this θ_{cm} angle distribution for all proton energies, not just the 800 MeV used at LAMPF.

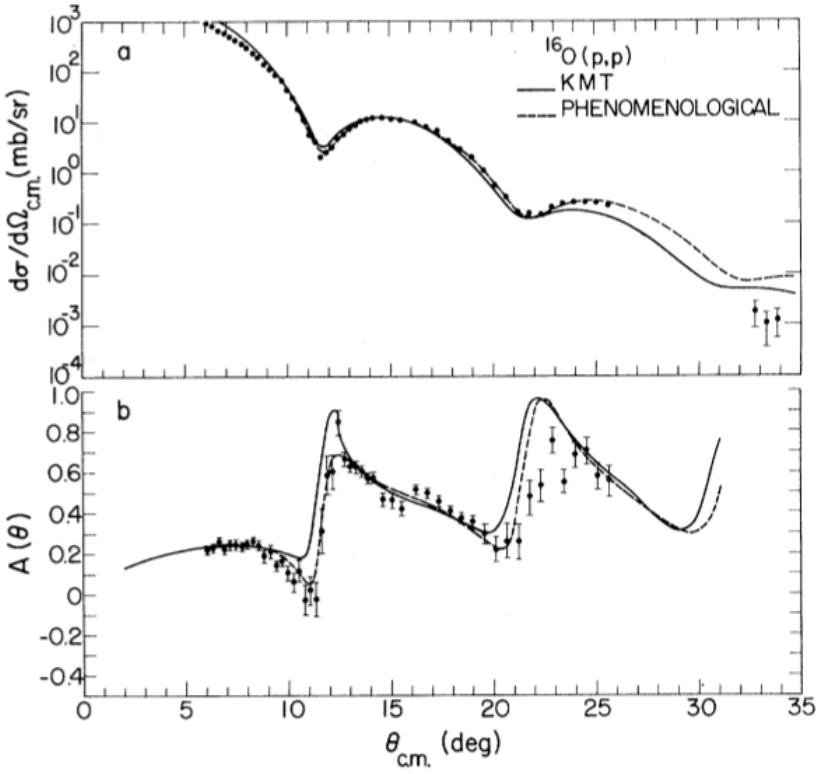

Figure 25: The θ_{CM} distribution from an experiment performed on ^{16}O in an 800 MeV, single energy proton beam. Differential cross sections and optical model fit for elastic scattering are shown in the upper panel. (The "analyzing power" A (θ) does not concern us) Statistical uncertainty are smaller than the data points unless otherwise indicated. No data exists below six degrees because that puts the detector too close to the beam. [3]

3.1 Scattering Algorithm

To use this center of momentum angular distribution it is necessary to conduct the simulated scattering while in the center of momentum frame. Thus, the procedure for simulated elastic scattering involves boosting from the laboratory frame to the center of momentum frame, conducting the scattering using some geometric prescriptions and finally boosting back out to the lab frame. Then the scattered hadron and remnant nucleus are passed to other parts of the simulation.

Four tests are performed on the scattering function to ensure it works. In this chapter the new scattering algorithm is debugged in pieces. These unit-tests are meant to be able to easily catch any problems with the code.

3.2 Center Of Momentum Calculations

The simulated elastic scatter starts with two four-vectors in the lab frame. $\vec{P_1}$ is the proton and $\vec{P_2}$ is the residual ^{11}C nucleus,
$\vec{\mathbf{P}}_1 = (E_1, p_{1x}, p_{1y}, p_{1z})$ and $\vec{\mathbf{P}}_2 = (E_2, p_{2x}, p_{2y}, p_{2z})$.
Then in the CM (primed) frame,

$$\vec{\mathbf{P}}_1^{'} = \mathbf{L}\vec{\mathbf{P}}_1 \tag{15}$$

where $\mathbf{L}$ is the Lorentz boosting matrix, a matrix of space-time rotations.

It requires one parameter, the vector velocity of one frame relative to the other $\frac{\vec{v}}{c} = \vec{\beta}$. This is the first step to generate these scattering events using a distribution of center of momentum scattering angles. To get $\vec{\beta}$ Given two particles with lab frame four-momenta P_1 and P_2, the four momentum of the pair

$$\vec{P_1} + \vec{P_2} = \left(\frac{E_1}{c} + \frac{E_2}{c}, \vec{p_1} + \vec{p_2}\right). \tag{16}$$

The center of momentum frame is defined as the frame in which the system's total momentum is zero

$$0 = \vec{p_1} + \vec{p_2} \tag{17}$$

This tells us that the system's total momentum has to be "shared" equally among

both particles in the CM frame. We may solve for the boost velocity and perform the CM frame transformation. The result is

$$\vec{\beta} = \frac{\vec{p_1} + \vec{p_2}}{E_1 + E_2} \tag{18}$$

Then $\vec{\beta}$ is used to calculate the individual the new components of momentum and energy in the CM frame for both particles. For the case where β is a boost in one dimension only the Lorentz equations for momentum and energy look like

$$E_i^{'} = \gamma \left(E_i - p_i c\beta \right) \tag{19}$$

$$p_i^{'} = \gamma \left(p_i - \beta E_i \right) \tag{20}$$

where i=1,2 for proton and ^{11}C nucleus

The full version is a complicated matrix, a more complex set of equations, indicating the appropriate spacetime rotations to produce a boost in an arbitrary direction. We use the implementation in the ROOT software, but validate it against several simpler test cases. [11]

$$\begin{bmatrix} ct' \\ x' \\ y' \\ z' \end{bmatrix} = \begin{bmatrix} \gamma & -\gamma\beta_x & -\gamma\beta_y & -\gamma\beta_z \\ -\gamma\beta_x & 1+(\gamma-1)\frac{\beta_x^2}{\beta^2} & (\gamma-1)\frac{\beta_x\beta_y}{\beta^2} & (\gamma-1)\frac{\beta_x\beta_z}{\beta^2} \\ -\gamma\beta_y & (\gamma-1)\frac{\beta_y\beta_x}{\beta^2} & 1+(\gamma-1)\frac{\beta_y^2}{\beta^2} & (\gamma-1)\frac{\beta_y\beta_z}{\beta^2} \\ -\gamma\beta_z & (\gamma-1)\frac{\beta_z\beta_x}{\beta^2} & (\gamma-1)\frac{\beta_z\beta_y}{\beta^2} & 1+(\gamma-1)\frac{\beta_z^2}{\beta^2} \end{bmatrix} \begin{bmatrix} ct \\ x \\ y \\ z \end{bmatrix}.$$

Figure 26: Lorentz transformation to another frame where $\vec{\beta}$ and γ are defined. This transformation applies also to $[E, p_x, p_y, p_z]$. By inspection it gives 3.5 and 3.6 when β_y, β_z are zero.

3.2.1 Case 1: Nucleus At Rest

The first test case for the boost where the proton probe has some random, physically realizable momenta and the nucleus is at rest. Here we expect the velocity in the center of momentum frame, or the boost, to be in the same direction as the only particle moving in the lab frame. The magnitude of proton momentum will be smaller in the Center of Momentum frame because all of the system's x,y, and z momenta in the lab frame are split between both particles in the CM frame.

$$p_1 = (\frac{E_1}{c}, \vec{p_1}) \tag{21}$$

$$p_2 = (m_2 c, \mathbf{0}) \tag{22}$$

$$\vec{p_1} + \vec{p_2} = (\frac{E_1}{c} + m_2 c, \vec{p_1}) \tag{23}$$

$$\vec{\beta} = \frac{\vec{p_1} + \vec{0}}{E_1 + m_2 c^2} \tag{24}$$

So β is in the direction of p_1 (Figure 27), but is smaller than the velocity of particle 1. The β velocity is a lot smaller if m_2 is much heavier than particle 1. And since this is now a one-dimensional problem, p_1, p_1' and p_2' will all be along the same line.

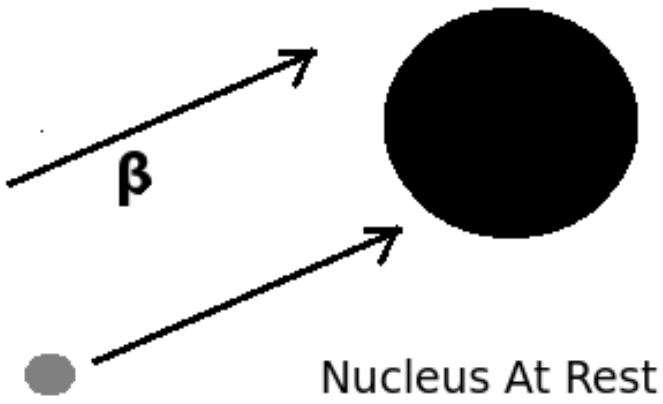

Figure 27: Figure above shows a proton with some momentum colliding with a nucleon at rest and the direction of $\vec{\beta}$

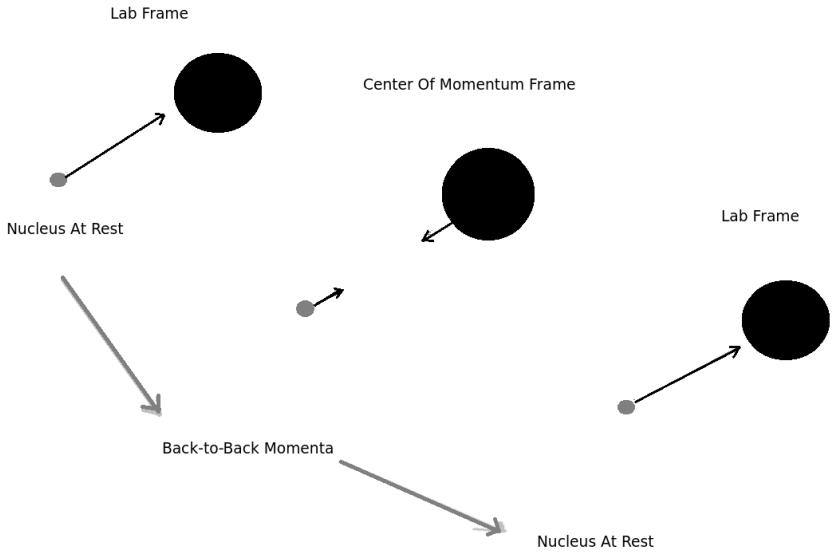

Figure 28: a proton with some momentum colliding with a nucleon at rest and how it appears in the center of momentum frame, but kinetic energy changes

Table 1 shows momentum and energy in both lab and CM frames for a sample event. Momentum in the CM frame is smaller because all of the momentum in the lab frame comes from the proton and must be "shared" with the nucleus (Figure 28). But it is in the same direction. Energy in the CM frame is smaller for the proton and larger for the nucleus. In the CM frame the particles are back-to-back. The magnitude of β is 0.0296623 and γ is 1.00044

Table 1: Boost Into/Out of Center Of Mass Frame (no scattering) Results

Case	Particle	P$_{x,y,z}$L	E_L	P$_{x,y,z}$CM	E_{CM}
1	Proton	0.212, 0.246, -0.072	0.995	0.194, 0.225, -0.066	0.986
1	^{11}C nucleus	0.0, 0.0, 0.0	10.26	-0.194, -0.224, 0.066	10.26

3.2.2 Case 2: Both Particles Already in CM frame

Case 2, shown in Figure 30, asks how a transformation to center of momentum performs on a system already in such a frame. So the boost should do nothing. But having the boost do nothing also allows us to easily see any inconsistencies quickly via GENIE's output.

```
 Check Angle 1.5708
AFTER THETA ROTATION---P3CM  P3CMmag 0.344558 P3CMxyz 0.33711 -0.0142901 0.0698059 E3CM 0.999535
Z-Axis CHECK------ -0 0 0.344558
P3CM 0.344558
AFTER PHI ROTATION---P3CM  P3CMmag 0.344558 P3CMxyz 0.33711 -0.0142901 0.0698059 E3CM 0.999535
Opening Angle 0
P3CMmag 0.344558 P3CMxyz 0.33711 -0.0142901 0.0698059 E3CM 0.999535
AFTER BOOST BACK---P3Lab 0.344558 P3Labxyz 0.33711 -0.0142901  0.0698059 E3Lab 0.999535
 E4CM calc 10.2598
P4CMmag 0.344558 P4CMxyz -0.33711 0.0142901 -0.0698059 E4CM 10.2598
Check CM-4-momentum conservation -  Energy  0, x momentum 0,    y momentum  0,    z momentum  0
AFTER BOOST BACK---P4Lab 0.344558 P4Labxyz -0.33711 0.0142901  -0.0698059 E4Lab 10.2598
BOOST BACK---- P1Lab  P1Labmag 0.344558 P1Lxyz 0.33711 -0.0142901 0.0698059 E1L 0.999535
BOOST BACK---- P2Lab  P2LabMag 0.344558 P2Lxyz -0.33711 0.0142901 -0.0698059 E2L 10.2598
Check 4-momentum conservation -  Energy  0, x momentum 0,    y momentum  0,    z momentum  0
 RemnP4 infoxyz before0.034615 0.0993614 0.0364195 10.2546
 AFTER 2-BODY KINEMATICS CALL----------------------------------------------------------------------------------------------------------------------------------
-------------------------------------------------------------------
 Mass of Particle 0.93827Mass of A 10.254Cos(theta_cm)--- 1
 t4PpL 0.33711 -0.0142901 0.0698059
 t4PtL -0.33711 0.0142901 -0.0698059
 t4P3L protonNewMomentum 0.33711 -0.0142901 0.0698059
 t4P4L nucleusNewMomentum -0.33711 0.0142901 -0.0698059
 fRemnP4 0.034615 0.0993614 0.0364195
 t4P3L 0.33711 -0.0142901 0.0698059
1560131957 NOTICE gevgen : [n] <gEvGen.cxx::GenerateEventsAtFixedInitState (311)> : Generated Event GHEP Record:

|-----------------------------------------------------------------------------------------------------------------------------------------------|
|GENIE GHEP Event Record [print level:   3]                                                                                                     |
|-----------------------------------------------------------------------------------------------------------------------------------------------|
| Idx |          Name | Ist |        PDG |   Mother  | Daughter  |      Px |      Py |      Pz |       E |      m  |                    |
|-----------------------------------------------------------------------------------------------------------------------------------------------|
|   0 |         nu_mu |   0 |         14 |  -1 |  -1 |   4 |   4 |   0.000 |   0.000 |   3.000 |   3.000 |   0.000 |                    |
|   1 |           C12 |   0 | 1000060120 |  -1 |  -1 |   2 |   3 |   0.000 |   0.000 |   0.000 |  11.175 |  11.175 |                    |
|   2 |       neutron |  11 |       2112 |   1 |  -1 |   5 |   5 |  -0.035 |  -0.099 |  -0.036 |   0.920 | **0.940 | M = 0.913          |
|   3 |           C11 |   2 | 1000060110 |   1 |  -1 |   7 |   7 |   0.035 |   0.099 |   0.036 |  10.255 |  10.254 |                    |
|   4 |           mu- |   1 |         13 |   0 |  -1 |  -1 |  -1 |  -0.372 |  -0.085 |   2.894 |   2.921 |   0.106 | P = (0.127,0.029,-0.991)
|   5 |        proton |  14 |       2212 |   2 |  -1 |   6 |   6 |   0.337 |  -0.014 |   0.070 |   1.000 |   0.938 | FSI = 3            |
|   6 |        proton |   1 |       2212 |   5 |  -1 |  -1 |  -1 |   0.258 |  -0.011 |   0.053 |   0.975 |   0.938 |                    |
|   7 |      HadrBlob |  15 | 2000000002 |   3 |  -1 |  -1 |  -1 |  -0.337 |   0.014 |  -0.070 |  10.260 | **0.000 | M = 10.254         |
|   8 |      NucBindE |   1 | 2000000101 |  -1 |  -1 |  -1 |  -1 |   0.079 |  -0.003 |   0.016 |   0.025 | **0.000 | M = -0.077         |
|-----------------------------------------------------------------------------------------------------------------------------------------------|
|       Fin-Init:                                                 |  -0.372 |  -0.085 |  -0.106 |   0.005 |                                |
|-----------------------------------------------------------------------------------------------------------------------------------------------|
|_      Vertex:          nu_mu @ (x =     0.00000 m, y =     0.00000 m, z =     0.00000 m, t =    0.000000e+00 s)  |
```


Figure 29: GHEP event record for case where both particles are in CM frame. Proton and nucleus before interaction are already back to back. Boost does nothing.

Looking at Equations 21 and 22, $\beta = 0$ because the already back-to-back vectors p_1 and p_2 sum to zero. Equivalently, for a single object (even a compound object like the proton and nucleus) β is defined as v/c and in the center of momentum frame that single object is at rest. Since $\beta = 0$, the definition Equation 18 leads to $\gamma = 1$ and therefore Equations 19 and 20 trivially yield unchanged E' and p' for both particles. Table 2 shows an example from a manipulated GENIE record.

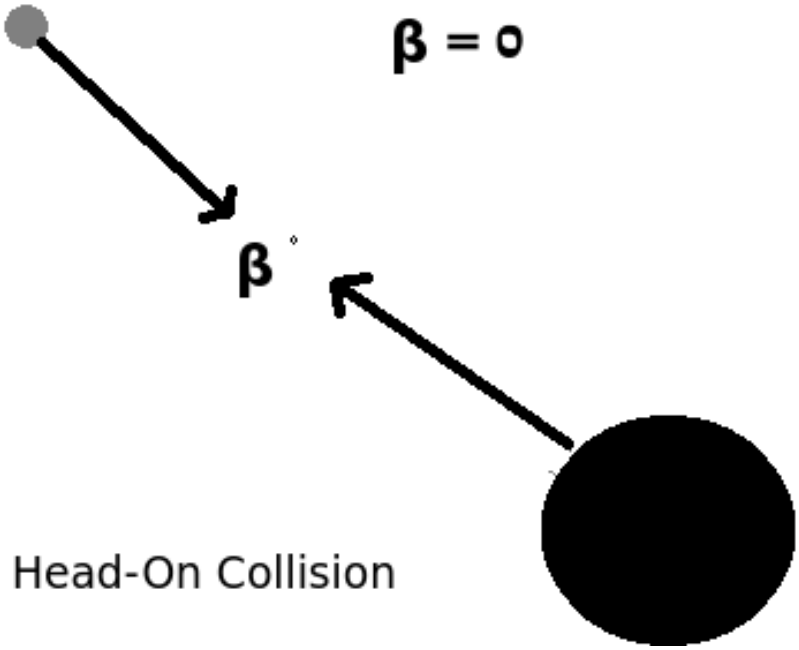

Figure 30: Proton and remnant nucleus colliding head to head already in Center of Momentum frame.

Table 2: Boost Into/Out of Center Of Mass Frame (no scattering) Results

Case	Particle	$P_{x,y,z}$L	E_L	$P_{x,y,z}$CM	E_{CM}
2	Proton	0.337 -0.014, 0.0698	0.999	0.337, -0.014, 0.0698	0.999
2	^{11}C	-0.337, 0.014, -0.069	10.26	-0.337, 0.014, -0.069	10.26

3.2.3 Case 3: Orthogonal Collision

In this last simple test case proton and nucleus have the same 3-momentum magnitude oriented orthogonal to one another. This should produce a β in both x and y-directions with no component in the z-direction in the lab frame. See Figure 31.

In the CM frame (Figure 32), both particles must be back to back by definition. No motion in the z-direction in the lab frame means that there is also no motion in z in the CM frame. This also means that the magnitude of proton momentum should be smaller in the CM frame. We are using the full 3D Lorentz boost from the ROOT software, but this is simple enough so we can anticipate the result.

In Table 3, the system's total momentum in the CM frame must be zero, both particles are back to back. The heavy nucleus means most of the momentum is in the x direction.

Table 3: Boost Into/Out of Center Of Mass Frame (no scattering) Results

Case	Particle	$P_{x,y,z}$L	E_L	$P_{x,y,z}$CM	E_{CM}
3	Proton	-0.703, 0.0, 0.0	1.173	-0.632 -0.070, 0.0	1.134
3	^{11}C	0.0, 0.703, 0.0	10.28	0.632 0.071, 0.0	10.28

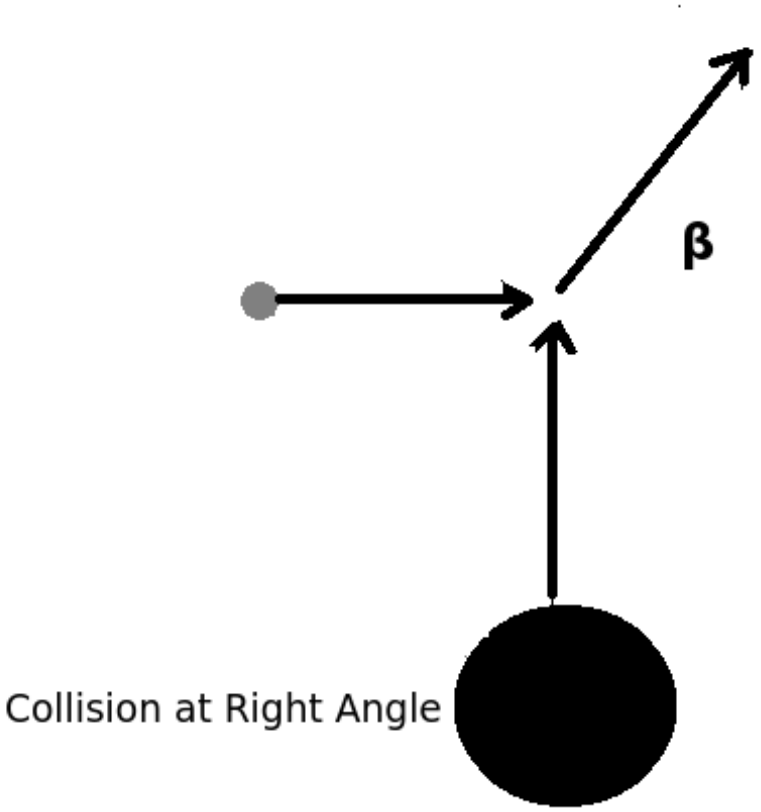

Figure 31: Figure above shows proton and remnant nucleus colliding at 90 degree angles

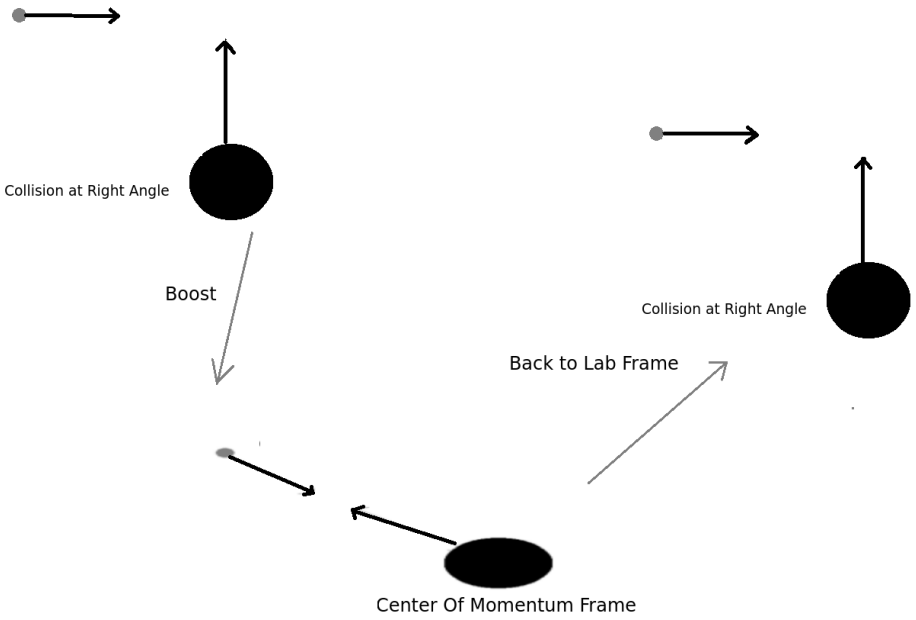

Figure 32: Figure above shows proton and remnant nucleus colliding at 90 degree angles

3.2.4 Case 4: Typical Event

In this test case the probe and remnant nucleus move in any random directions (Figure 33) that GENIE might generate. In a typical event the probe and nucleus will head towards one another. It can and does happen that the particles are heading in the same direction. They still collide because the nucleon starts inside the nucleus. Here

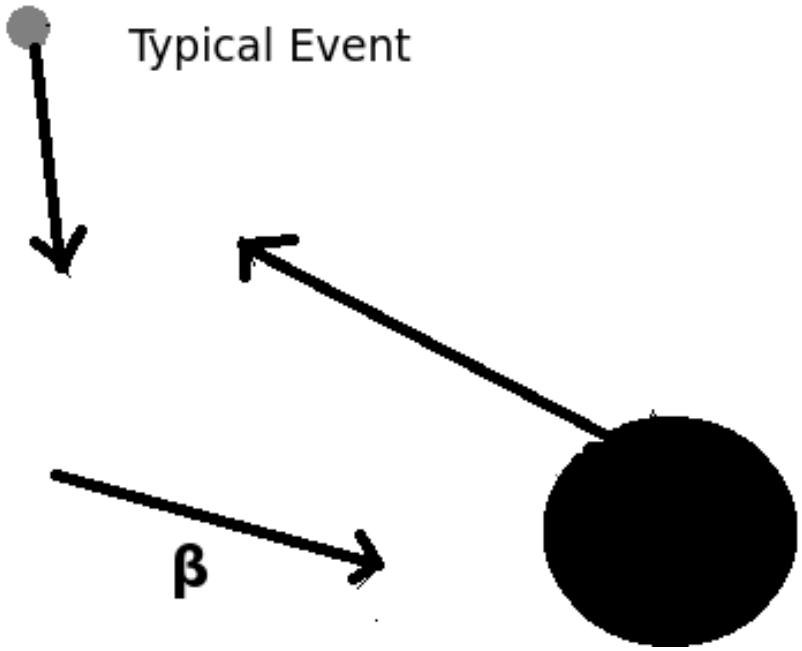

Figure 33: Figure above shows proton and remnant nucleus colliding in a typical event

the full three dimensional boost routine in ROOT is needed. Except that the momenta in the CM frame is back to back (Figure 34) it is difficult to test for correctness quantitatively. But all the special cases pass validation so the general case does too.

In Table 4 output from GENIE shows one randomly selected event for each case. The lab and CM frames momenta and energies are shown for both particles.

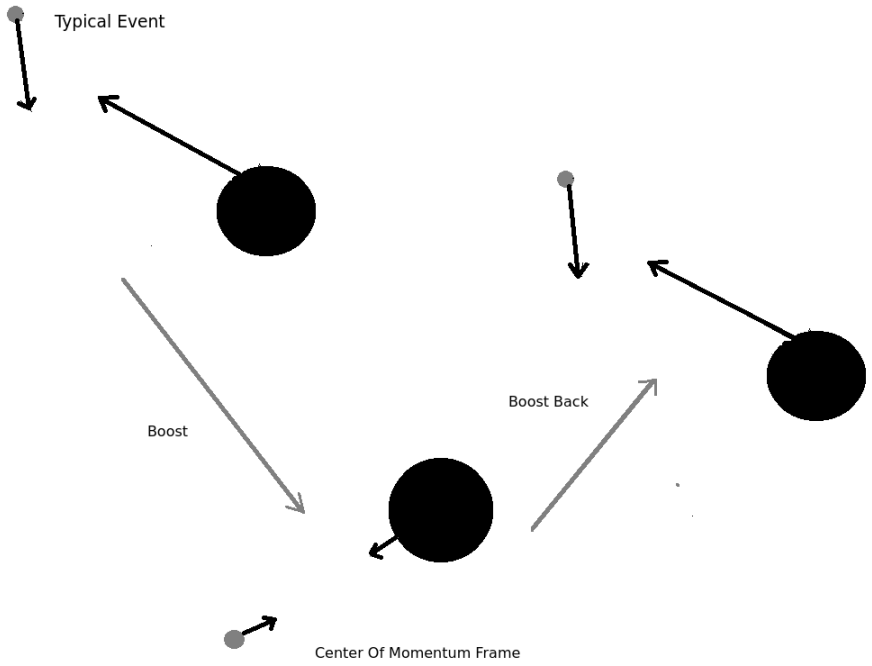

Figure 34: Figure above shows a typical collision event, boost to CM frame and boost back to lab frame

Table 4: Boost Into/Out of Center Of Mass Frame (no scattering) Results

Case	Particle	P$_{x,y,z}$L	E_L	P$_{x,y,z}$CM	E_{CM}
4	Proton	0.388, 0.328, 0.317	1.113	0.361 0.308, 0.295	1.093
4	^{11}C	-0.115, -0.115, -0.123	10.256	-0.3614, -0.308, -0.296	10.269

3.3 Testing Scattering Function

Scattering changes the direction of the particles in the center of momentum frame by some angle θ_{cm}, like shown in Figure 35. After the scatter the particles are still back-to-back and their energies are unchanged. The process for simulating such a scatter uses the measured distribution of scattered proton angle in the CM frame described earlier.

The full 3D scattering involves a rotation by θ_{cm} around any orthogonal vector followed by a random ϕ rotation around the original vector. Initially to test, the CM angle is set to zero, followed by the case where the CM momenta of both the remnant nucleus and the proton are along the z-axis. In the latter case the scattering reduces to a few equations.

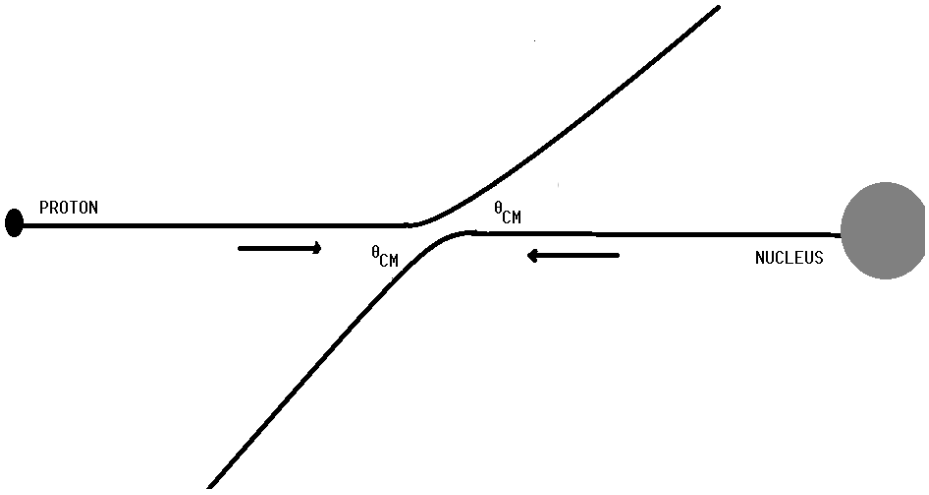

Figure 35: elastic scattering in CM frame. Zero scattering angle should produce no scattering interaction and unchanged momentum.

3.3.1 Test 1: $\theta_{cm} = 0$

In this case the nucleus is placed at rest and no scattering occurs. The proton emerges from the scattering with its momentum unaltered. The original code failed this test. Several iterations of my algorithm had trouble with it too. In Chapter 4 this test reveals additional implications beyond simple correctness of the algorithm.

Figure 37 shows the proton before reinteraction (status 14) changes direction after being measured outside the nucleus (status 1) in red. The expected behavior is the status 1 proton has the same direction , but lower momentum. This accounts for the 25 MeV cost to remove the bound proton from the nucleus.

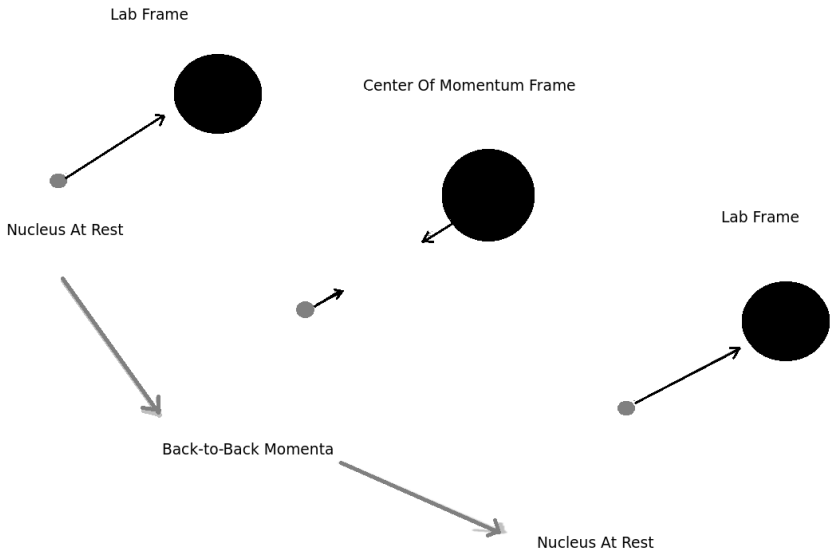

Figure 36: A proton with some momentum "colliding" with a nucleon at rest. Both proton and nucleus are back to back in the CM frame. They do not scatter and so continue along the same trajectory.

GENIE GHEP Event Record [print level: 3]

Idx	Name	Ist	PDG	Mother	Daughter	Px	Py	Pz	E	m
0	nu_mu	0	14	-1 -1	4 4	0.000	0.000	3.000	3.000	0.000
1	C12	0	1000060120	-1 -1	2 3	0.000	0.000	0.000	11.175	11.175
2	neutron	11	2112	1 -1	5 5	-0.035	-0.099	-0.036	0.920	**0.940
3	C11	2	1000060110	1 -1	7 7	0.035	0.099	0.036	10.255	10.254
4	mu-	1	13	0 -1	-1 -1	-0.372	-0.085	2.894	2.921	0.106
,-0.991)										
5	proton	14	2212	2 -1	6 6	0.337	-0.014	0.070	1.000	0.938
6	proton	1	2212	5 -1	-1 -1	0.249	0.057	0.071	0.975	0.938
7	HadrBlob	15	2000000002	3 -1	-1 -1	0.047	0.011	0.013	10.254	**0.000
8	NucBindE	1	2000000101	-1 -1	-1 -1	0.076	0.017	0.022	0.025	**0.000

Figure 37: Old Elastic code produces a proton whose direction changes despite not scattering. This is obviously incorrect.

3.3.2 Test 2: Momentum In CM frame along Z-Axis

In this case both the proton and remnant nucleus are set to have momenta along the z-axis in the center of momentum frame. See Figure 38. This provides a special limiting case to check.

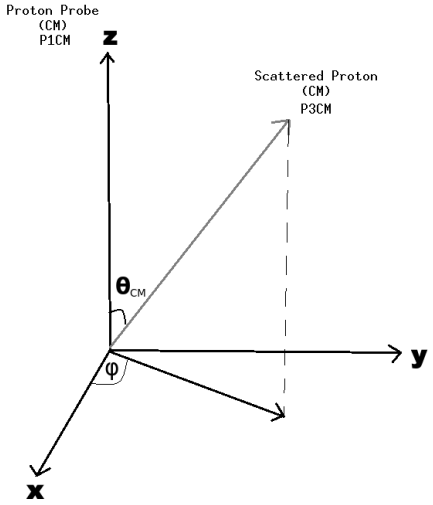

Figure 38: Figure above shows a proton with only z momenta scattered by some angle θ_{cm}.

In this case the scatter occurs through a rotation of a vector away from the z-axis. This case is a straightforward calculation to check.

So the 4-momentum of the scattered proton is

$$\begin{aligned} E_3^{'} &= E_1^{'} \\ P_{3x}^{'} &= P_1^{'} * sin\theta * cos\phi \\ P_{3y}^{'} &= P_1^{'} * sin\theta * sin\phi \\ P_{3z}^{'} &= P_1^{'} * cos\theta \end{aligned} \tag{25}$$

If θ and ϕ are known, these equations will give yield the p_x, p_y, p_z.

The convention we use here is that subscripts 1 and represent the proton while subscripts 2 and 4 represent the nucleus. The primed superscript still represents the CM frame while the unprimed the lab frame. So P_{1cm} or P_1' is the proton's momentum before scattering in the CM frame. P_{3cm} or P_3' is the proton's momentum after scattering in the CM frame. $E_{1cm}(E_{3cm})$ or $E_1'(E_3')$is the proton's energy in the CM frame before (after) scattering.

These Equations in 25 should match the consecutive rotations made using the ROOT software rotation functions. The first around the y-axis, down to the xy-plane by θ. The second rotation occurs around the z-axis (which was the original direction) by a randomly chosen ϕ between 0 and 2π.

The plan is to use existing rotation routines in ROOT and check them using these formulas for this special case. After this, I apply the rotations also to the remnant ^{11}C nucleus. Or simply set its momentum to be exactly the opposite of the proton. They both give the same answer, but the latter is faster for the computer.

3.3.3 Test 3: Momentum in CM frame along Y-axis

The solution used here for a particle on the z-axis (rotation around the y-axis) only works for vectors in the x-z plane. By changing the motion to the y or x-axis, we see the need for an additional case. If the momentum is along the y-axis then obviously the rotation cannot be done around that axis. We must rotate around a vector orthogonal to our original momentum vector.

The concept is simple to understand by analogy to a simpler case. Consider a vector in 2D space. If we want to rotate it some angle θ in the xy plane we need only rotate the vector around the z-axis by θ. The most general orientation of a 3D vector requires the general case treatment which follows. However, our strategy for choosing the orthogonal vector must carefully account for all possible input directions.

3.3.4 Test 4: Arbitrary Momentum

We expect the system's momentum in the CM frame could be along any direction. This configuration will examine the algorithm's ability to handle cases where momenta

in the CM frame appears along one axis, not just the z-axis. The algorithm will choose the simplest vector perpendicular to our proton's momentum in the CM frame. The dot product between the original vector and the orthogonal vector will be zero. Of course, the dot product being zero is used to accomplish this while taking into consideration the zero components of the momentum vector.

Choose a random vector with components (x,y,z) and our proton P_1 with components (P_{1x}, P_{1y}, P_{1z}) in the center of momentum frame. We want a vector perpendicular to P_1

$$(P_{1x}, P_{1y}, P_{1z}) \cdot (x, y, z) = 0 \tag{26}$$

$$P_{1x} \cdot x + P_{1y} \cdot y = -P_{1z} \cdot z \tag{27}$$

$$\vdots$$

$$z = -\left(\frac{P_{1y} \cdot y + P_{1x} \cdot x}{P_{1z}}\right) \tag{28}$$

Assume P_{1z} is nonzero. Then one component (here I choose x) may be set to 0 and the other (y) to one. This new vector with components $(0, 1, \frac{P_{1y}}{P_{1z}})$ is by definition orthogonal to our original proton CM vector. Then the original vector is rotated around the derived orthogonal vector by the GENIE-sampled scatter angle theta. Finally an angle ϕ is chosen at random and the rotated proton is rotated once again by ϕ around the original vector. We expect the result to be independent of the chosen ϕ, but this step is crucial to make sure that the scattered vector is isotropic in ϕ.

```
  PHI3 = 2*Pi * rnd -> RndFsi().Rndm();
 //check if P1CM is in x-y plane special cases
if(TMath::Abs(P1CM.Z())< 0.00001){
    if(TMath::Abs(P1CM.Y())>.00001){
        OrthoVec.SetXYZ(1,-P1CM.X()/P1CM.Y(),0);}
    else if(TMath::Abs(P1CM.Y()) <.00001){
    OrthoVec.SetXYZ(-P1CM.Z()/P1CM.X(),0,1);
    }
    }
else{
```

```
//Create a vector orthogonal to P1CM common case
    OrthoVec.SetXYZ(0,1,-(P1CM.Y())/P1CM.Z());
    }
//Rotate proton in CM frame around OrthoVec
P3CM.Rotate(theta, OrthoVec);
```

By default input the simple perpendicular vector is anchored in the yz plane. But if the arbitrary momentum has zero z component (along the x-axis for example) this will not work. Here we need to make sure that the denominator in the last equation is nonzero. So this particle cannot have a zero center of momentum x-momentum. So we make a special case for no or very small z components.

These are cases in the xy-plane. If the particle is near the y-axis we may choose x=1 and z=0. Otherwise we choose y = 0 and z = 1 in which case the particle is on the x-axis and we rotate around a vector in the xz plane. In the code fragment above, we trap these special cases first and most input protons fall through to the third and most general case.

4 Results

4.1 New Transverse Kinematic Distributions

This chapter will cover the new algorithm's effects on each of the transverse kinematic quantities. Then we explore some more extreme scattering angles to poke at the features of each distribution. Finally, a recommendation is made for how to incorporate the fixed elastic into MINERvA's analysis.

The artifacts of the original code are gone. Overall changes to the transverse kinematic distributions are pretty drastic. Populations that appeared to distort the QE peak have shifted mostly to the peak and other events have dropped out of the measurement sample altogether.
In most cases fixed elastic FSI behaves approximately like the no FSI events. There are mild effects due to the prevalence of small angle scattering. The ratio of elastic to no FSI events is presented to highlight this. Most plots through section 4.4 have a lower panel with the flat ratio indicates that the elastic and no FSI distributions have the same shape. The region at the edge of the peak contains a distortion in this ratio, but this is expected since small angle scattering causes those events which to migrate out of the peak into the tail.

4.1.1 Coplanarity Angle $\delta\phi_T$

In Figure 39 coplanarity, the quantity which measures how out of the neutrino-muon plane is the proton as it exits the nucleus, has noticeable changes to its elastic piece. Originally the elastic portion piled up at very small coplanarity angles. They were easily distinguished from the rest of the FSI sample. With the new elastic code those events appear similar events with no FSI.

Recall that the proton gets its transverse momentum from the transverse motion of the struck neutron and a second struck nucleon during reinteraction. The old elastic code's preferentially coplanar proton momenta indicate that either the proton has very small momenta to begin with or the struck nucleus had very small momenta. This was not the case, instead it was a design flaw in the originial code.

The lower panel shows how similar elastic FSI is to no FSI. The white population in the upper panel, no-FSI, has transverse momentum from Fermi motion alone. Any deviations from the white population shape are due to the particular artifacts of that FSI fate. Left of the peak the ratio of elastic to no FSI is pretty steadily 0.48. The nearly flat ratio indicates that the behavior of these elastic protons in that region have the same out-of-the-planeness as a proton only undergoing Fermi motion.

Just beyond the peak around 15 degrees the ratio increases. Some elastic events in the peak have moved to the right. Since these events moved into a region where they had not been previously, this increases the ratio of elastic to no FSI a region. The increase is large because there were few events there to begin with.

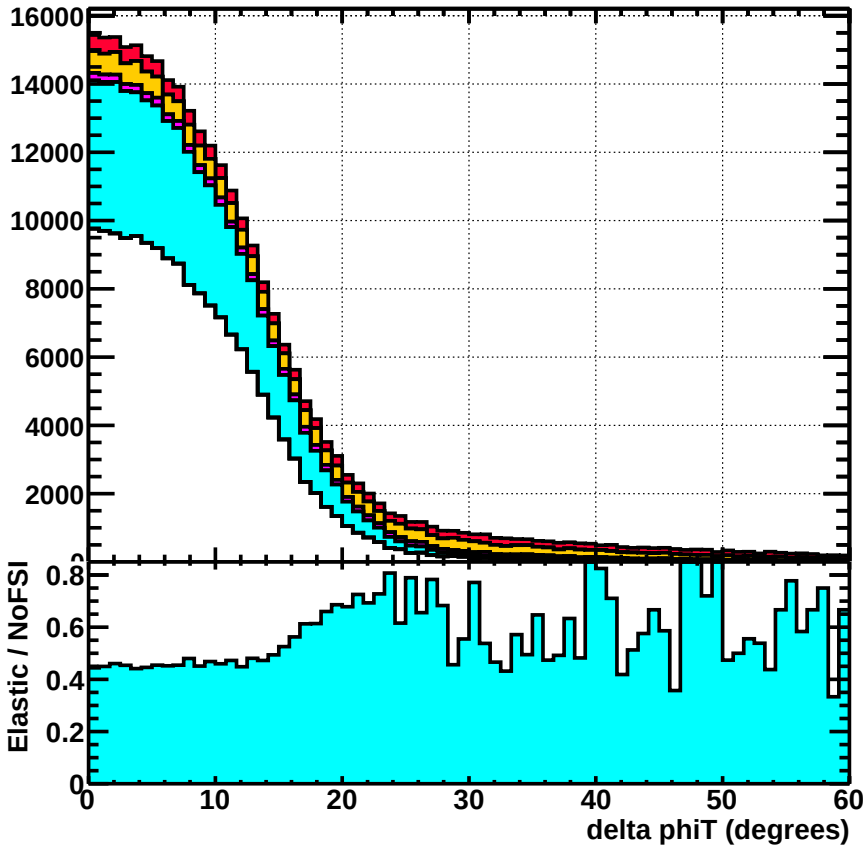

Figure 39: New $\delta\phi_T$ distribution. Compare to Figure 20. The lower panel shows the ratio of elastic to no FSI events. TThe ratio is flat everywhere except the region just beyond the peak.

4.1.2 Transverse Momentum Transfer δP_T

δp_T measures the proton's departure from a non-FSI no-Fermi motion event in units of momentum. The white portion of this plot again represents the transverse momentum of the neutron before the neutrino's initial W interaction. The old elastic distribution showed (Figure 21) a pileup of events at low momentum meaning elastic events produced more protons with even less momentum than protons with only Fermi motion. These now have a similar pattern to the no-FSI events.

The ratio of elastic to no FSI is almost flat around 0.48. The elastic piece looks like no-FSI in the region just before the peak below 0.18 GeV. Beyond the peak the ratio increases due to events migrating into the tail. As before, the small angle scatters are adding many events to a portion of the spectrum that had few to begin with.

The other FSI fates have a mostly flat distribution. The elastic and no FSI fates are decreasing in this region because they only experience Fermi gas motion. Therefore the other fates dominate the tail of the distribution.

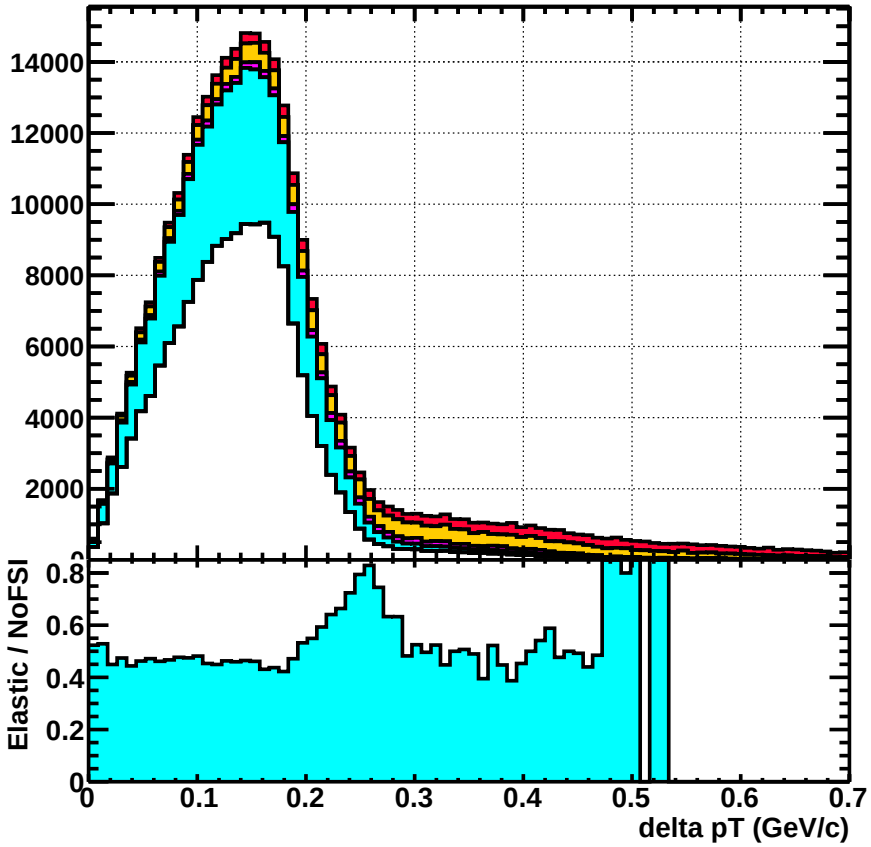

Figure 40: New δP_T distribution Compare to Figure 21. The lower panels shows the ratio of elastic to no FSI events. The ratio is flat everywhere except the region just beyond the peak.

4.1.3 "Acceleration Angle" $\delta\alpha_T$

The acceleration angle $\delta\alpha_T$ previously had a large population of elastic events below 40 and above 160 degrees. The white portion is the distribution due to just Fermi motion. Fermi motion is just as likely to make the proton appear accelerated as decelerated so the white distribution is nearly isotropic. The other three fates preferentially lower the proton momentum and show decelerated $\delta\alpha_T$ near 180 degrees.

The new $\delta\alpha_T$ the elastic portion appears very nearly isotropic. The ratio of elastic to no-FSI is 0.48. Because this distribution is intrinsically flat, the small angle scatters migrate events every way and no peak appears in the ratio like the previous plots. The other FSI fates all produce lower energy protons. They seem "decelerated" and appear closer to 180 degrees.

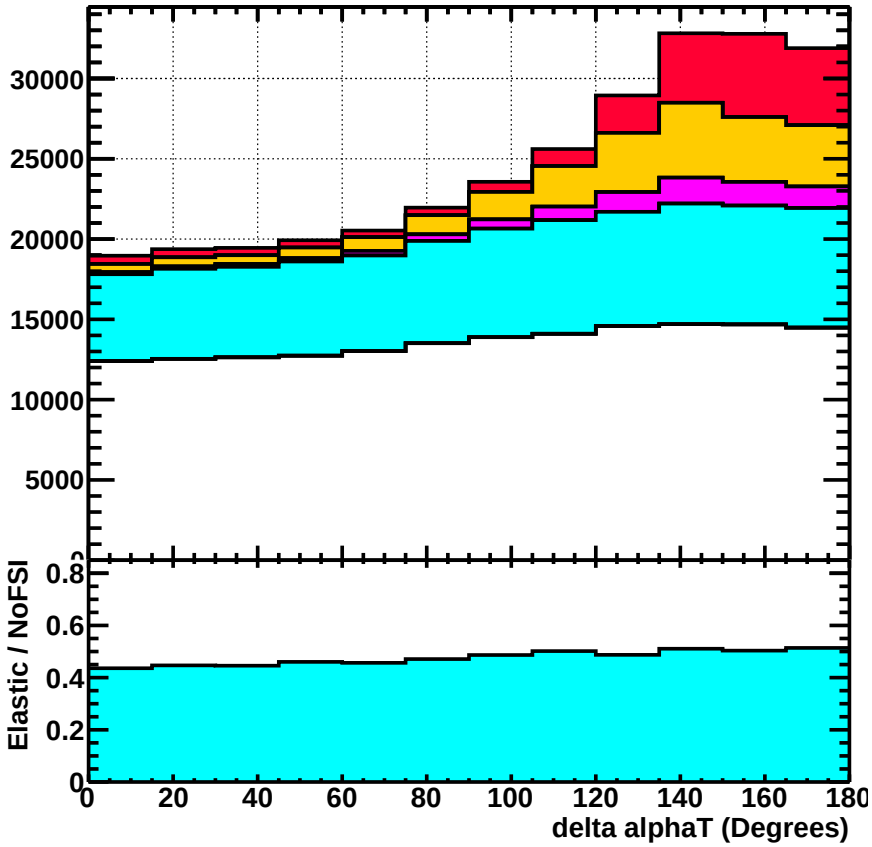

Figure 41: New $\delta\alpha_T$ distribution. Compare with Figure 22.The lower panels shows the ratio of elastic to no FSI events. The ratio is flat throughout.

4.1.4 CCQE Inferred Neutron Momentum P_n

In the new elastic scattering P_n, the initial neutron momentum distribution, no longer shows standout features. The old plot showed a large number of events with especially small momenta. This meant that the elastic scatter proton had less momentum than those having undergone just Fermi motion.

The new elastic events are very similar to no FSI events. The ratio of elastic to no FSI is flat around 0.48. This flat ratio indicates that the shapes of both distributions is the same. Near the edge of the peak (above 0.226 GeV/c) events that have migrated out of the peak and into this region cause the ratio to increase.

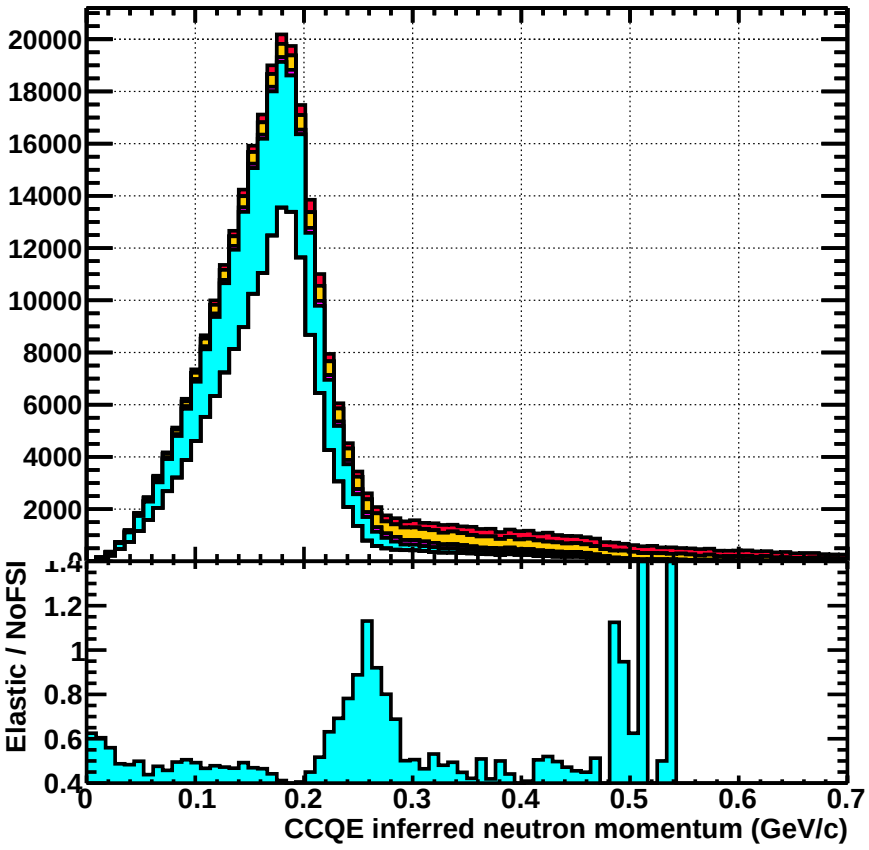

Figure 42: New P_n distribution. Compare to Figure 23. The lower panels shows the ratio of elastic to no FSI events. The ratio is flat everywhere except the region just beyond the peak.

With the elastic FSI fixed and the artifacts gone, this distribution and δP_T are of special interest. They allow us to evaluate how well we model the Fermi motion and the energy cost to remove a nucleon from the nucleus. See Figure 11. The removal energy uncertainties produce a bias in the outgoing proton momentum that shifts the peak. Adding more energy to the nucleus to free a nucleon reduces the proton energy and shifts or broadens many of the kinematic imbalance quantities.

5 Analysis and Recommendations

5.1 Exaggerated Center Of Mass Angles

In order to figure out which parts of the distributions are most sensitive elastic FSI events are generated with a single center of momentum scatter angle. These angles are picked to be more extreme than the GENIE sampled scatter angles. Most of the original center of mass angles are around 2 or 3 degrees. Beginning with a larger five degree angle and an even more extreme 25 degree angle, gives a useful visualization about how these change the new distributions.

All four distributions for a uniform five degree scatter are shown in Figure 47. In the lower panels of each plot large differences may be seen in the region just at the edge of the peak. In the GENIE chosen angles the ratio of elastic to no FSI is about 1.2 while in the forced 5 degree scatter plot shows a larger ratio of 1.8. Considering the baseline is 0.48 these effects carry a factor of 2 or 3 at that spot in the distribution. This indicates that even at 5 degrees there is a more prominent event migration away from the peak. This effect is small, but may be measurable. It specifically looks like a widening of the peak when compared to the nominal angle distribution.

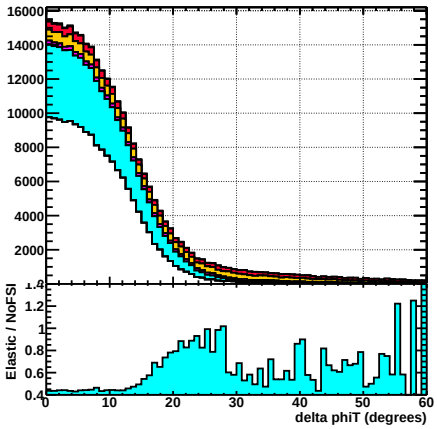

Figure 43: New Coplanarity Angle $\delta\phi_T$ θ_{cm}=5

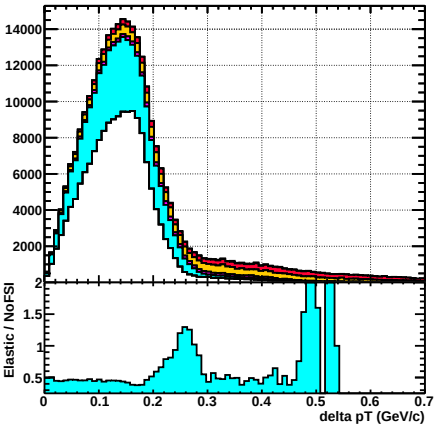

Figure 44: New P_n θ_{cm}=5

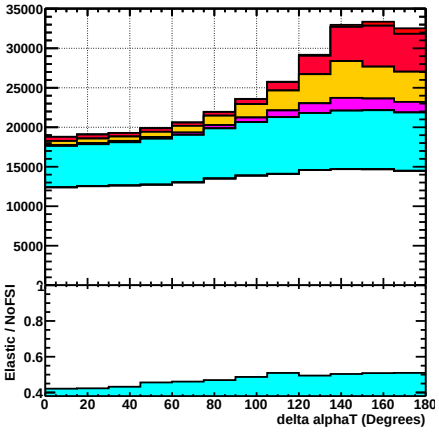

Figure 45: New "Accelerating Angle" $\delta\alpha_T$ θ_{cm}=5

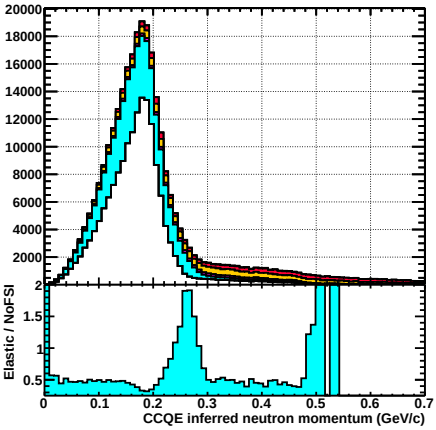

Figure 46: New P_n θ_{cm}=5

Figure 47: All events are generated with scattering angle θ_{cm}= 5 degrees a) Coplanarity Angle $\delta\phi_T$ b) Transverse momentum imbalance δp_T c) Accelerating Angle $\delta\alpha_T$ d) Inferred Neutron Momentum p_n

On the other hand the forced 25 degree scatter angle has features that differ substantially from the distributions produced using GENIE's chosen angles. There is a severe increase in events in the tail. In this region the ratio of elastic to no FSI events is very large because we shifted almost all the elastic events into a region that had few to begin with.

Figure 48 - 51 all show that large angles fall in the tail region of the distribution and are a severe deviation from the no scatter case. In Figure 50 the extreme angle makes the elastic portion in $\delta\alpha_T$ anisotropic.

This effect is large enough that the difference between the 5 degree enhancement, the nominal, and no enhancement may be measurable. As described in Section 3.1 the amount of scattering is taken from 800 MeV ^{16}O proton beam data, and has large uncertainties. Some FSI models do not include this process at all.

The takehome here is that any nonzero scattering angle used to simulate elastic scattering pushes events into the tail region, effectively broadening the elastic peak. Any attempt to circumvent the arduous process of applying the code fix requires understanding GENIE's nominal angles are very small and produces an elastic distribution not too different from no FSI.

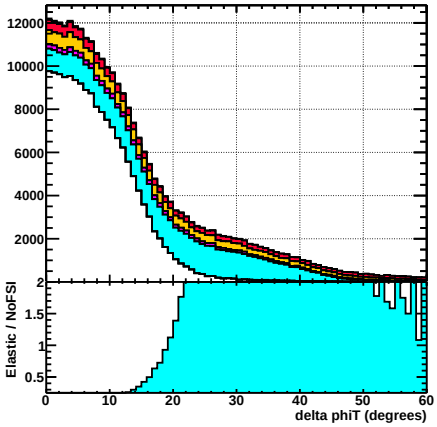

Figure 48: New Coplanarity Angle $\delta\phi_T$ θ_{cm}=25

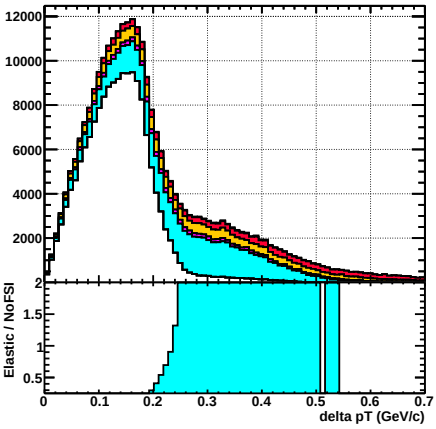

Figure 49: New P_n θ_{cm}=25

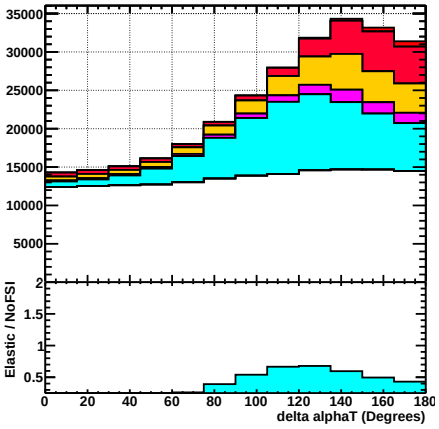

Figure 50: New "Accelerating Angle" $\delta\alpha_T$ θ_{cm}=25

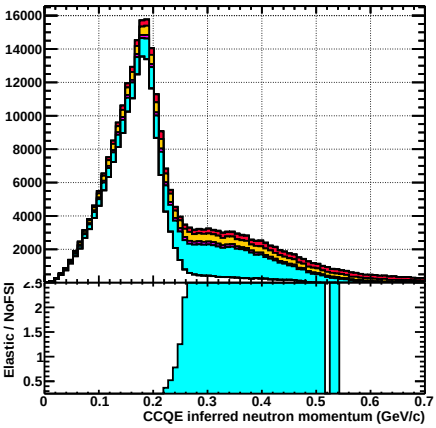

Figure 51: New P_n θ_{cm}=25

Figure 52: All events are generated with scattering angle θ_{cm}= 25 degrees a) Coplanarity Angle $\delta\phi_T$ b) Transverse momentum imbalance δp_T c) Accelerating Angle $\delta\alpha_T$ d) Inferred Neutron Momentum p_n

5.2 Center of Momentum Scatter Angle Set to Zero

Since a scatter angle of zero means both particles continue along the same trajectory it presents a useful extreme for study. This zero scatter angle is really no FSI. Looking at the plots of the transverse variables the ratio of elastic to no FSI events is about 0.48 everywhere. The flat ratio indicates that the elastic (with no scattering) has the same shape as the no FSI portion of the distribution, exactly what is expected. This is a way to show the effects in the previous section really are from the θ_{cm} and not from a selection effect.

Elastic FSI events without scattering look like no FSI, as expected. The ratio of elastic to no FSI for coplanarity is very nearly flat throughout the distribution. The two populations have the same shape. The δp_T transverse momentum imbalance, p_n, and $\delta\alpha_T$ all have the same basically flat ratio of 0.48. The only deviation appears to be $\delta\alpha_T$ in that its ratio of elastic to no FSI events is even flatter. It is a flat distribution to begin with so this is also expected.

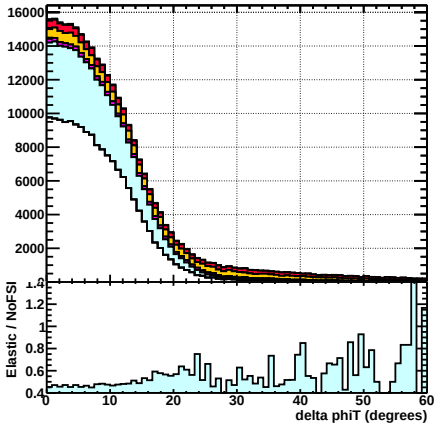

Figure 53: New Coplanarity Angle $\delta\phi_T$ θ_{cm}= 0

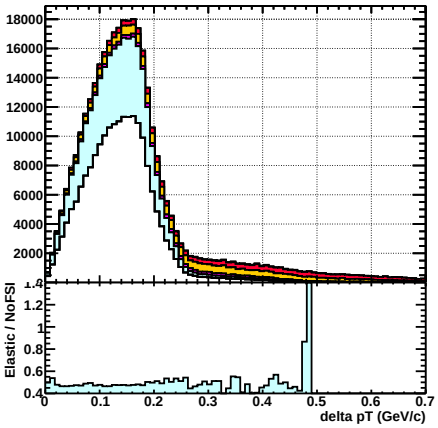

Figure 54: New P_n θ_{cm}=0

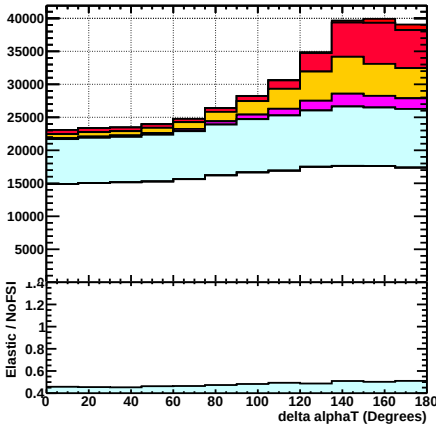

Figure 55: New "Accelerating Angle" $\delta\alpha_T$ θ_{cm}=0

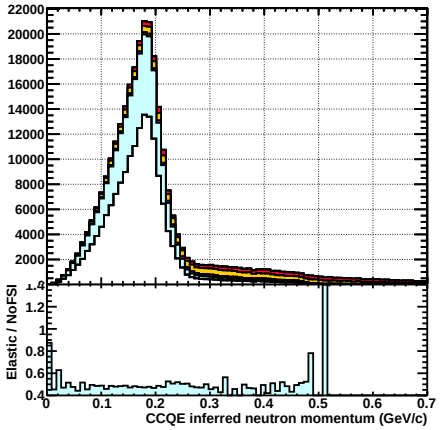

Figure 56: New P_n θ_{cm}=0

Figure 57: All events are generated with θ_{cm}= 0 a) Coplanarity Angle $\delta\phi_T$ b) Transverse momentum imbalance δp_T c) Accelerating Angle $\delta\alpha_T$ d) Inferred Neutron Momentum p_n

5.3 Acceleration

Turns out the acceleration in Figure 24 was a red herring. It was only an artifact of the error in the code. In Figure 58 the change in kinetic energy is centered about zero, meaning the proton is just as likely to accelerate as it is to decelerate after scattering off the nucleus. This is typical of random elastic scattering, of which most familiar is thermal motion of an ideal gas leading to the Maxwell velocity distribution. [21]

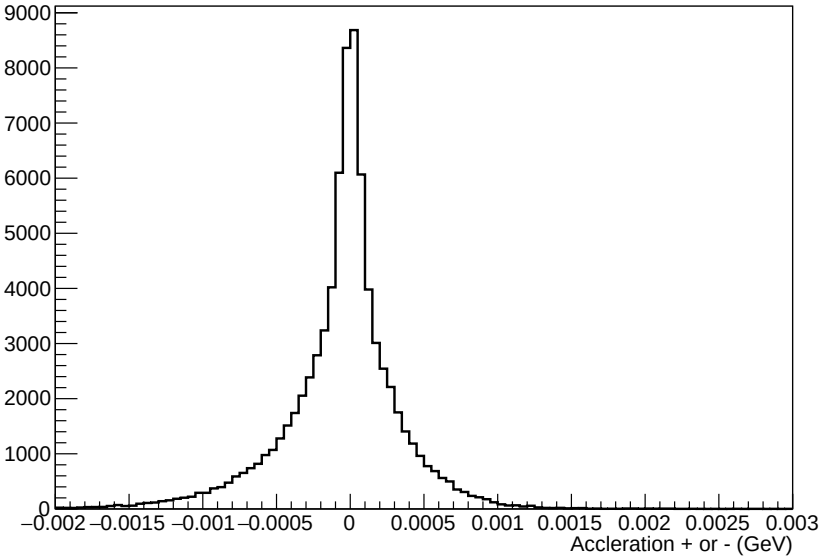

Figure 58: New elastic FSI change in kinetic energy after scatter shows protons are equally accelerated and decelerated after scatter. The distribution is centered about zero just as we would expect.

Even the old (incorrect) accelerations were only 2 MeV. Uncertainties in the energy cost to remove a nucleon as well as the detector energy scales are larger than this. So the old 2 MeV bias is not an issue for analysis of hadronic energy-it is just too small.

5.4 Measurement Cuts

GENIE will predict every possible event, but the experiment cannot measure all of those events. For this reason limits or "cuts" are placed to avoid certain immeasurable or unrealistic values. For the muon produced with the primary interaction of the W boson cuts are place at 1.5 GeV and 10.0 GeV. In addition, muon angles smaller than 20 degrees are not accepted. For the final state proton only momenta between 450 MeV and 1.2 GeV are considered while only proton-neutrino beam angles less than 70 degrees can be measured.

In addition to changing the four transverse kinematic quantities, the old elastic scattering code allowed too many events to pass the selection cuts. Below is a table which tracks the number of events for each FSI fate after successive "cuts" are made on the muon and proton final state particles. Note that the acceptance ratio for the old and new elastic scattering processes are close with just over half of events accepted by the proton momentum cuts (second line). However, the proton-beam angle cuts show that the new elastic retains more than 40 percent of the sample while the old kept 50 percent.

Table 5: **FSI Fate After Successive Cuts** *(Event Acceptance Rate After Cut)*

Cuts	**Old Elastic**	**Fixed Elastic**	**No FSI**
muon only	195,815	194,033	259,918
	(.8769)	*(.8786)*	*(.7263)*
muon +	100,594	99,937	200,051
proton momentum	*(.514)*	*(.515)*	*(.767)*
muon +	97,642	78,115	163,317
proton momentum +			
proton angle	*(.4986)*	*(.4026)*	*(.6283)*
Cuts	**Charge Exchange**	**Inelastic**	**Knockout**
muon only	36,674	87,124	133,570
	(.7589)	*(.7697)*	*(.7979)*
muon +	12,580	35,100	30,137
proton momentum	*(.343)*	*(.403)*	*(.226)*
muon +	8432	24,778	21,165
proton momentum +			
proton angle	*(.6703)*	*(.7059)*	*(.7023)*

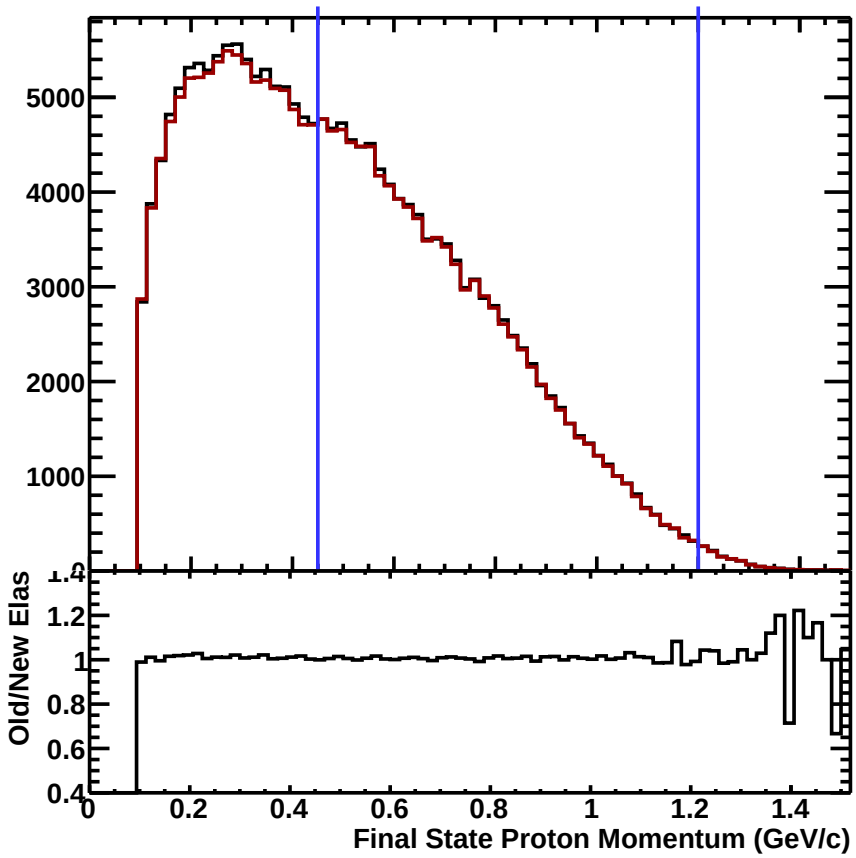

Figure 59: Ratio of Proton Angle for old elastic to New Elastic without Angle Cuts

Figure 59 shows the final State proton momentum for old and fixed elastic are very close as can be seen in the unity ratio between the two. This is not too surprising given the very small 2 MeV anomalous positive kinetic energy change present in the old elastic simulations. This 2 MeV amounts to roughly 5 MeV/c or 0.005 GeV/c in momentum, which explains the similar acceptance rate in the region of proton momentum cuts. That 2 MeV is just not enough to change that final state momentum distribution. This could be part of the reason the old elastic's inconsistencies were not noticed until the transverse variable distributions analysis.

Note that in Table 5 the acceptance rate for no-FSI fate is much higher than either elastic rates. This indicates that these FSI momentum distributions are energy dependent. Figure 62 shows old and new elastic and no FSI distrbutions with pro-

ton momentum cut boundaries indicating that the no-FSI portion peaks within the boundaries of the momentum cuts.

Multi-pion knockout, inelastic scattering, and charge exchange all show low acceptance (near 20 percent) rates for the muon cuts. Figure 60 shows proton momentum before momentum cuts for various FSI processes. For these processes the distribution peaks outside of the cut boundaries. Some like multinucleon knockout have very few events allowed into the measurement sample. Often the reinteraction reduces the proton energy and momentum so it no longer passes the momentum selection. The final breakdown of FSI events was shown in Figure 12. An experiment with a lower momentum threshold (like Argon TPCs) would retain more of these in the final sample than MINERvA.

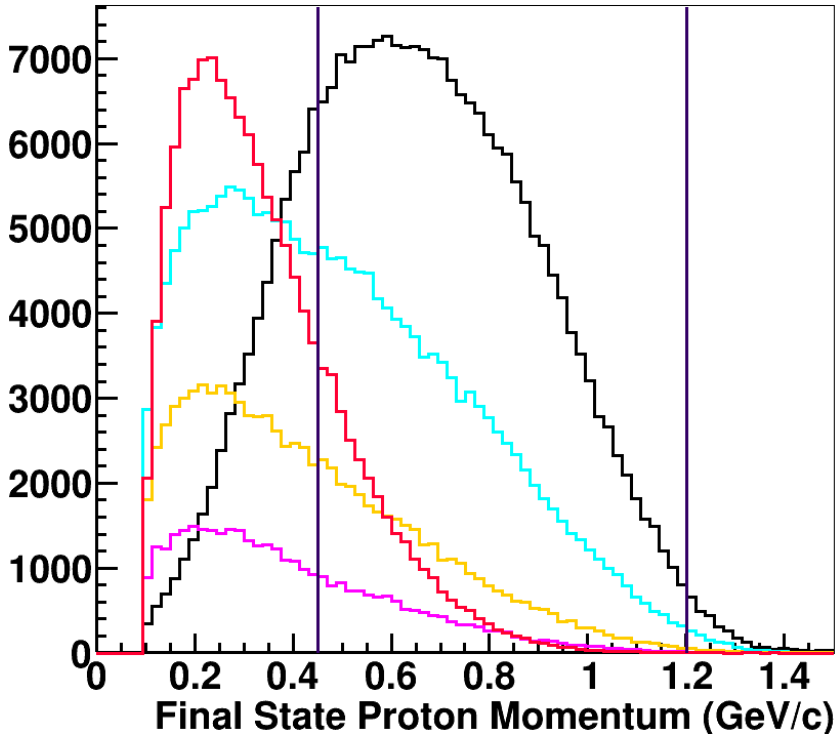

Figure 60: FSI fates proton momentum by fate black-no FSI, blue-elastic, red-charge exchange, yellow-inelastic, magenta-multi-nucleon knockout.

5.4.1 Proton Angle Measurement

The proton angle is the next successive cut after the muon and momentum cuts. Figure 61 shows the angle cuts on a final state proton after momentum cuts have already been applied. In the third row of Table 5 the acceptance rates for no FSI, old, and fixed elastic FSI fates are shown. This is where a clear change from old and new elastic FSI can be seen.

The new elastic FSI fate has a 20 percent lower acceptance rate. Figure 61 shows that the angular distribution for the old elastic FSI has fewer large angle events. This allows more events to make it through the angle measurement cuts.

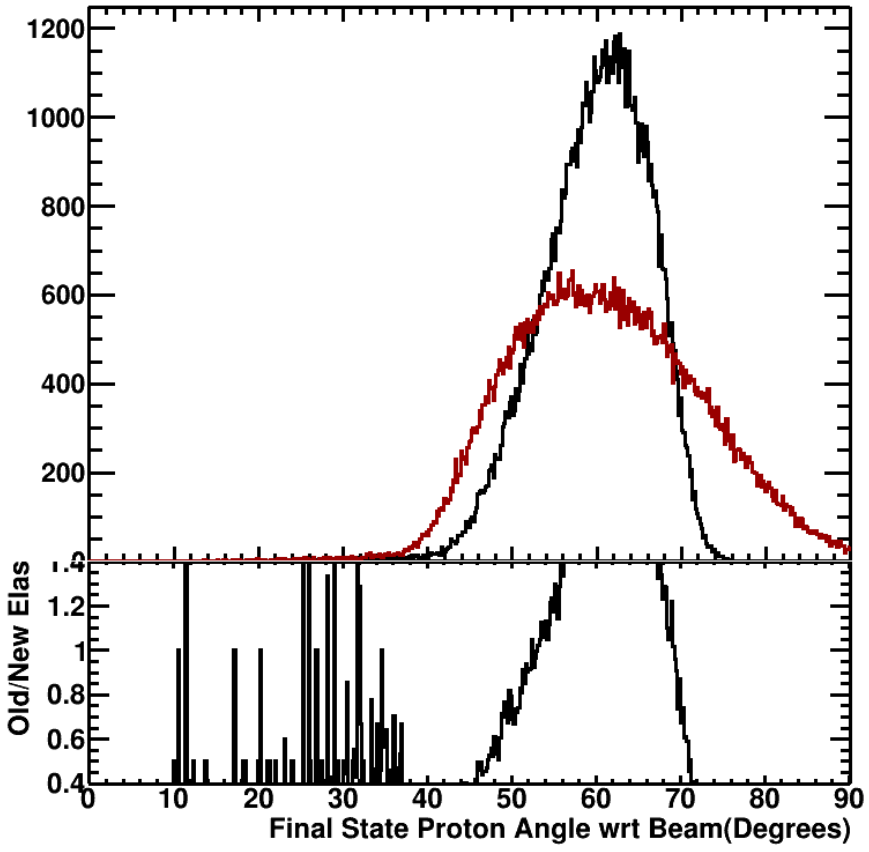

Figure 61: Proton Angle Measurement old vs new with Cuts at 0 and 70 degrees. The old elastic FSI (black) has a much narrower peak than the new elastic (red).

5.5 Simple Reweight

Since the new elastic code produces very different transverse kinematic distributions we need to correct this to proceed with MINERvA's analyses. Generating new MC samples in GENIE then processing them through the full detector simulation and event reconstruction is laborious. If we can reweight some already processed events and produce the same effect on the distribution that physics requires then we usually prefer to do that. This saves a lot of time and several person-months of effort.

The nearly constant ratio of elastic to no-FSI events provides an important clue for a reweighting procedure. A quick and approximate method would involve replacing all elastic events with no scatter, or no FSI events.

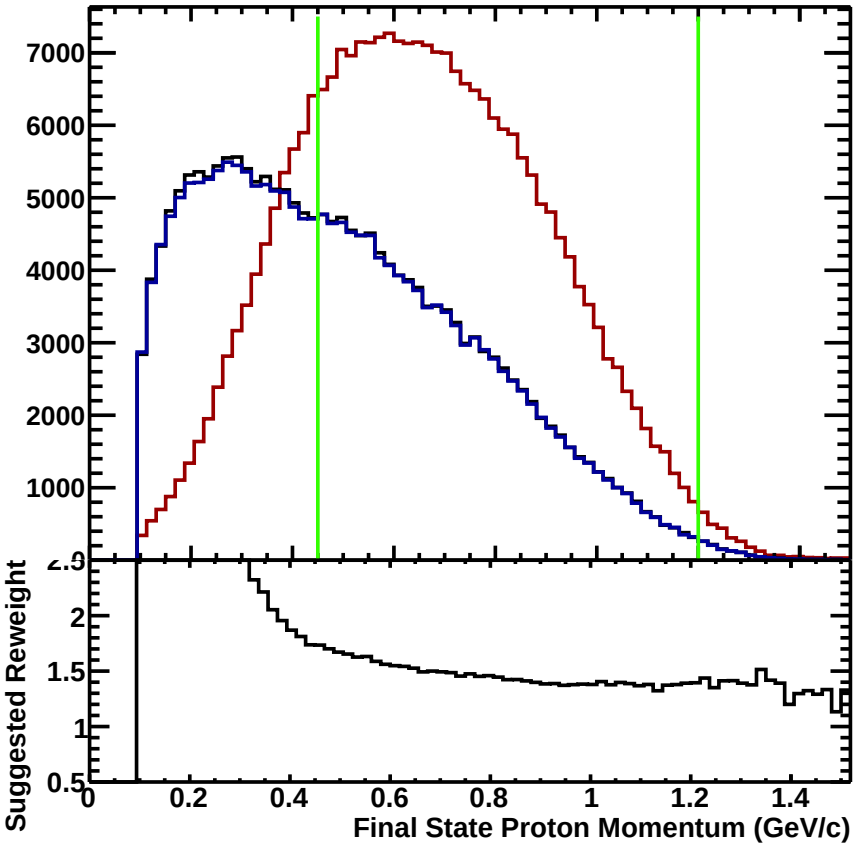

Figure 62: Proton Momentum illustrating a reweighting factor of 1.5 will work for the range within the cuts.

In this prescription all old elastic FSI events before the proton angle cuts are replaced my no FSI events at the same stage. In the second row of Table 5 there are old 100,594 elastic FSI events and 200,051 no FSI events. So I reweight the no FSI events to about 1.50284 and the elastic FSI events to zero. Figure 62 is the result of such a reweighting scheme.

If the momentum threshold were lower we would need an energy dependent weight. In Figure 59 the green lines are the cut boundaries. If the boundary was at a lower momentum the no FSI events are fewer than the new elastic. Only at around 0.3 GeV/c does the ratio of new elastic to no FSI events begin to stabilize.

Figure 67 shows the ratio of this reweighted to the zero scatter angle distribution. The two are identical as evidenced by the unity ratio in the lower panel. Using a single factor instead of an energy dependent weight is a good approximation for these events.

Basically, if the fixed elastic consisted of only zero scatter angles it would look exactly like the reweighed no FSI.

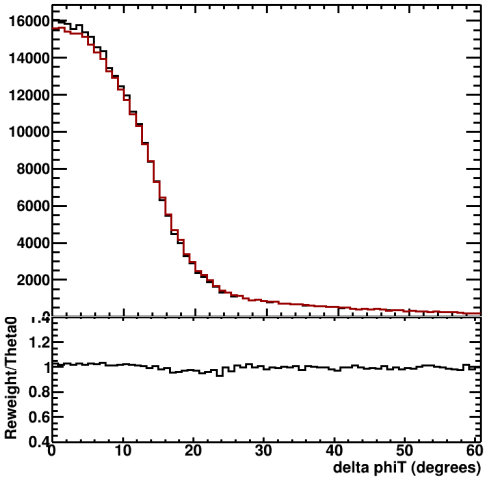

Figure 63: Coplanarity Angle $\delta\phi_T$ Ratio of reweighted to θ_{cm}=0

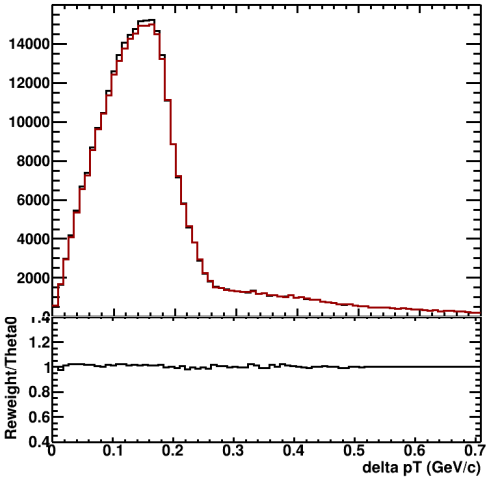

Figure 64: Transverse Momentum Transfer δp_T Ratio of reweighted to θ_{cm}=0

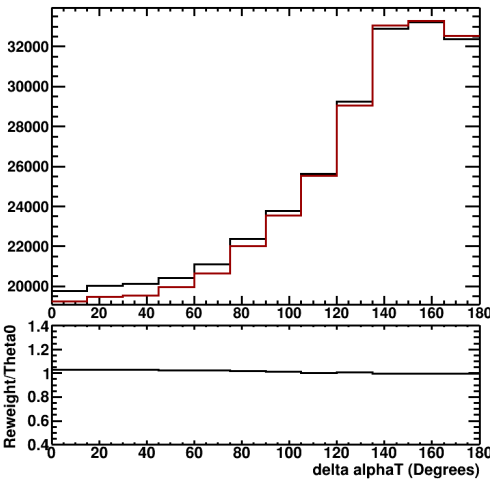

Figure 65: $\delta\alpha_T$ ratio of reweighted to θ_{cm}=0

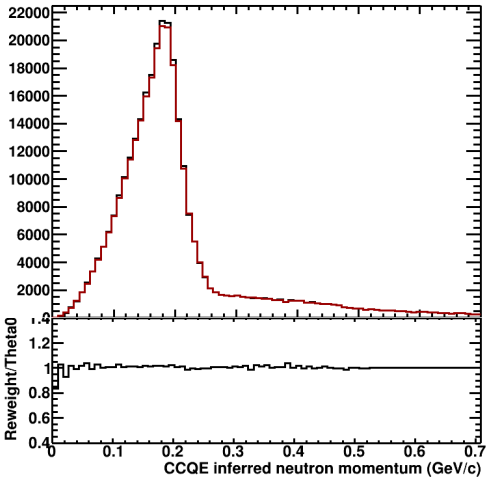

Figure 66: CCQE inferred neutron momentum P_n ratio of reweighted to θ_{cm}=0

Figure 67: Ratio of Reweight vs $\theta_{cm} = 0$. The ratio is within a few percent of one everywhere, the reweight is nearly perfect.

Next in Figure 72 the reweighted no-FSI is compared to the distributions where elastic is fixed. Here, once again the ratio is unity and only deviating slightly in the same region just beyond the peak. These random scatter angle events are not accounted for in the reweighting scheme by design. Saving the cost of regenerating fully simulated samples means we miss this feature of the prediction.

In parallel with completing this thesis, Tejin Cai (Ph.D student at University of Rochester), Xianguo Lu (postdoctoral researcher at University of Oxford) and Minerba Betencourt (scientist at Fermilab) implemented my prescription to reweight events. They used that to reextract the cross sections presented in [16]. Another artifact of the old code is that it had a detrimental affect on the extraction of the measured data points for the transverse kinematic cross sections. The new reweighting scheme shifted the data points substantially in places where the elastic FSI had a large distortion. The results are in MINERvA docdb 23382 [10] and are being prepared for publication.

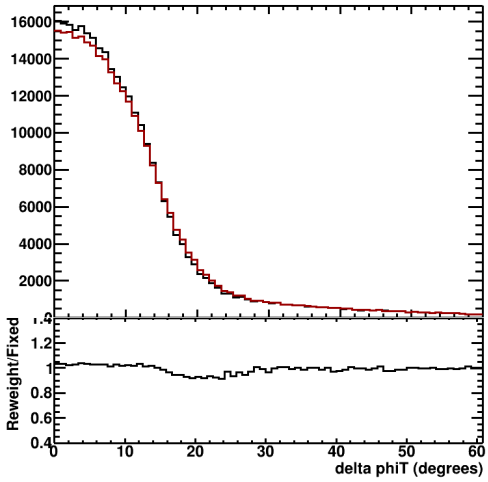

Figure 68: Coplanarity Angle $\delta\phi_T$ Ratio of reweighted to fixed elastic

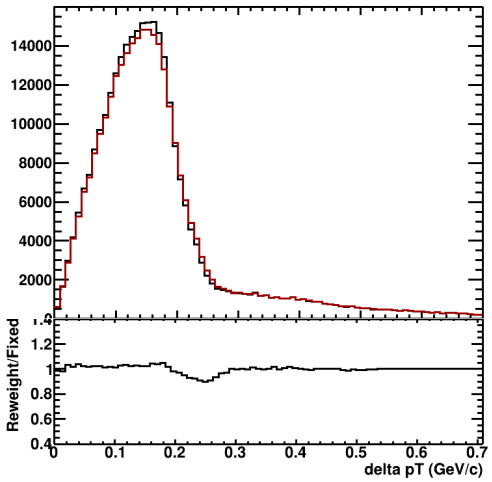

Figure 69: Transverse Momentum Transfer δp_T Ratio of reweighted to fixed elastic

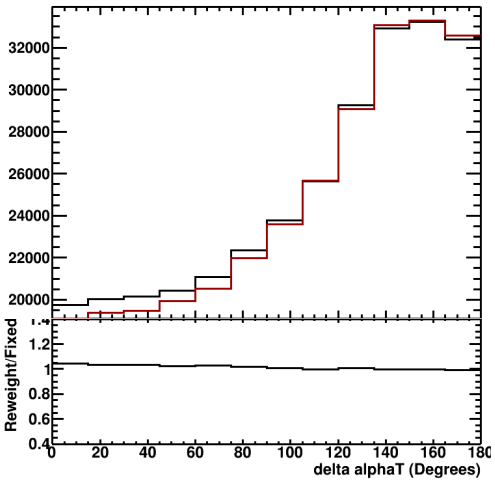

Figure 70: $\delta\alpha_T$ ratio of reweighted to fixed elastic

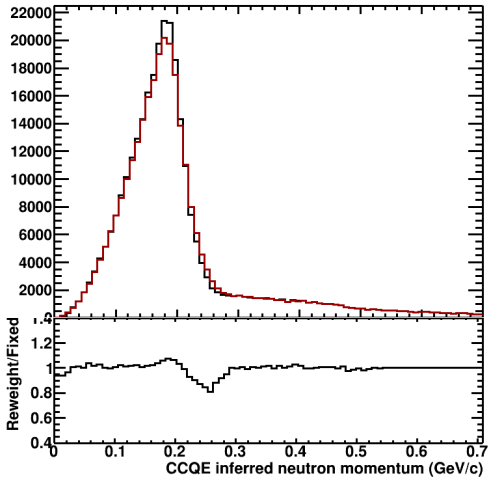

Figure 71: CCQE inferred neutron momentum P_n ratio of reweighted to fixed elastic

Figure 72: Ratio of Reweight vs Fixed

The fixed code described in this thesis also affects two-body inelastic scattering and charge exchange FSI, and the equivalent FSI for pions.

By extension, it affects nearly all processes simulated by GENIE. Dividing the effort, Tejin Cai and Trung Le (postdoctoral researcher at Tufts University) did some initial tests of these other processes, where the detrimental effects were smaller than for transverse kinematic imbalance studies. Conclusions from this thesis and a limited set of tests for other processes produced by Dr. Gran are collected in a public technical note to share with the four other neutrino experiments (NOvA, T2K, MicroBooNE, and DUNE) currently using this version of GENIE. This note is MINERvA internal document 23259 (MINERvA Technical Note 91) and are public on arXiv.org. The fixed code has been shared with the GENIE authors for evaluation and inclusion in an upcoming release.

6 Conclusion

Transverse kinematic distributions revealed oddities in the elastic scattering FSI model. In particular, the coplanarity angle $\delta\phi_T$ did not show expected Fermi motion effects. It was expected that when the center of momentum frame scattering angle was set to zero the proton should have exited the nucleus in roughly the same direction. Instead, the proton changed direction and was in many cases accelerated.

I wrote a new algorithm for GENIE's elastic scattering FSI which resulted in dramatic changes in the transvere kinematic variables. Now the elastic portion is very similar to a model where the proton does not reinteract. Analysis of these new distributions also revealed the difference between sample sizes in old and fixed elastic codes stemmed from the measurement cut acceptance rates. The old elastic FSI did not produce the number of large angle protons that should have been in the sample.

Developing a solution to correcting the wrong code's distributions and the impact they have on other MINERvA analyses would require regenerating millions of Monte Carlo events. This is arduous task.

An appropriate reweighting scheme has all elastic events are turned off and no FSI events are reweighted to recreate the number of events that the old elastic would have produced. The reweight was technically perfect as shown by the unity ratio of reweighted to zero CM angle distributions. However, it will not capture the random nonzero scatter angles that moved events from the peak into the tail.

References

[1] Home.

[2] *Elementary particle physics: revealing the secrets of energy and matter*. National Acad. Press, 1998.

[3] G. S. Adams, T. S. Bauer, G. Igo, G. Pauletta, C. A. Whitten, A. Wriekat, G. W. Hoffmann, G. R. Smith, M. Gazzaly, L. Ray, W. G. Love, and F. Petrovich. Microscopic description of 800-mev polarized-proton scattering from ^{16}O. *Phys. Rev. Lett.*, 43:421–424, Aug 1979.

[4] P. Adamson et al. The NuMI Neutrino Beam. *Nucl. Instrum. Meth.*, A806:279–306, 2016.

[5] L. Aliaga et al. Design, Calibration, and Performance of the MINERvA Detector. *Nucl. Instrum. Meth.*, A743:130–159, 2014.

[6] C. Andreopoulos, C. Barry, S. Dytman, H. Gallagher, T. Golan, R. Hatcher, G. Perdue, and J. Yarba. The GENIE Neutrino Monte Carlo Generator: Physics and User Manual. 2015.

[7] W. B. Atwood and G. B. West. Extraction of asymptotic nucleon cross sections from deuterium data. *Phys. Rev. D*, 7:773–783, Feb 1973.

[8] A. Bodek, M. E. Christy, and B. Coopersmith. Effective spectral function for quasielastic scattering on nuclei. *The European Physical Journal C*, 74(10):3091, Oct 2014.

[9] A. Bodek and J. L. Ritchie. Further Studies of Fermi Motion Effects in Lepton Scattering from Nuclear Targets. *Phys. Rev. D*, 24:1400, 1981.

[10] T. Cai. Effects on systematics after reweighting out elastic ha, minerva docdb 23382.

[11] CERN. Root.

[12] W. entry. Special relativity, 2019.

[13] W. entry. Standard model, 2019.

[14] R. J. Glauber. Theory of high energy hadron-nucleus collisions. In S. Devons, editor, *High-Energy Physics and Nuclear Structure*, pages 207–264, Boston, MA, 1970. Springer US.

[15] R. Gran. The MINERvA neutrino interaction experiment. *AIP Conf. Proc.*, 981(1):256–258, 2008.

[16] X. Lu. Neutrino shadow play: Kinematic determination of nuclear effects at minerva, minerva docdb 17864. 2018.

[17] X. G. Lu et al. Measurement of final-state correlations in neutrino muon-proton mesonless production on hydrocarbon at $\langle E_\nu \rangle = 3$ GeV, MINERvA DocDb 17864. *Phys. Rev. Lett.*, 121(2):022504, 2018.

[18] A. I. M. H.-O. P. Physics. Beta decay, 2019.

[19] G. RDEL and R. BEYER. Neutrino electron scattering. *Modern Physics Letters A*, 08(12):1067–1088, 1993.

[20] D. D. Stancil et al. Demonstration of Communication using Neutrinos. *Mod. Phys. Lett.*, A27:1250077, 2012.

[21] S. S. Wong. *Introductory Nuclear Physics*. Wiley-VCH Verlag GmbH Co. KGaA, Strauss GmbH, Morlenbach, second edition edition, 2004.